

AFRL-VS-TR-2003-1547

---

**INSTALLATION AND OPERATION OF PARTICLE TRANSPORT  
SIMULATION PROGRAMS TO MODEL THE DETECTION AND  
MEASUREMENT OF SPACE RADIATION BY SPACE-BORNE  
SENSORS**

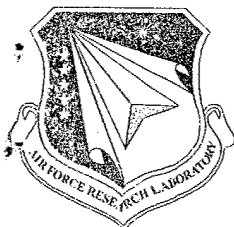
**Stanley Woolf**

**ARCON CORPORATION  
260 Bear Hill Road  
Waltham, MA 02451-1080**

**6 February 2003**

**Scientific Report No. 3**

**APPROVED FOR PUBLIC RELEASE; DISTRIBUTION UNLIMITED**



**AIR FORCE RESEARCH LABORATORY  
Space Vehicles Directorate  
29 Randolph Rd  
AIR FORCE MATERIEL COMMAND  
Hanscom AFB, MA 01731-3010**

---

**20030812 047**

This technical report has been reviewed and is approved for publication.

Bronislaw K. Dicht

Contract Manager

[Signature]

Branch Chief

This document has been reviewed by the ESC Public Affairs Office and has been approved for release to the National Technical Information Service.

Qualified requestors may obtain additional copies from the Defense Technical Information Center (DTIC). All others should apply to the National Technical Information Service.

If your address has changed, if you wish to be removed from the mailing list, or if the addressee is no longer employed by your organization, please notify AFRL/VSIM, 29 Randolph Rd., Hanscom AFB, MA 01731-3010. This will assist us in maintaining a current mailing list.

Do not return copies of this report unless contractual obligations or notices on a specific document require that it be returned.

# REPORT DOCUMENTATION PAGE

Form Approved  
OMB NO. 0704-0188

Public Reporting burden for this collection of information is estimated to average 1 hour per response, including the time for reviewing instructions, searching existing data sources, gathering and maintaining the data needed, and completing and reviewing the collection of information. Send comment regarding this burden estimates or any other aspect of this collection of information, including suggestions for reducing this burden, to Washington Headquarters Services, Directorate for Information Operations and Reports, 1215 Jefferson Davis Highway, Suite 1204, Arlington, VA 22202-4302, and to the Office of Management and Budget, Paperwork Reduction Project (0704-0188,) Washington, DC 20503.

1. AGENCY USE ONLY ( Leave Blank)

2. REPORT DATE

February 6, 2003

3. REPORT TYPE AND DATES COVERED

Interim Scientific Report #3  
01 Aug. 2001 - 31 July 2002

4. TITLE AND SUBTITLE Installation and Operation of Particle Transport Simulation Programs to Model the Detection and Measurement of Space Radiation by Space-borne Sensors

5. FUNDING NUMBERS

F19628-99-C-0077  
PR - 2822  
TA - GC  
WU - AR

6. AUTHOR(S)

Dr. Stanley Woolf

7. PERFORMING ORGANIZATION NAME(S) AND ADDRESS(ES)

ARCON Corporation, 260 Bear Hill Rd., Waltham, MA 02451-1080

8. PERFORMING ORGANIZATION REPORT NUMBER

9. SPONSORING / MONITORING AGENCY NAME(S) AND ADDRESS(ES)

Air Force Research Laboratory  
29 Randolph Road  
Hanscom AFB, MA 01731-3010  
AFRL Contract Manager: Dr. Bronislaw K. Dichter, AFRL/VSBXR

10. SPONSORING / MONITORING AGENCY REPORT NUMBER

AFRL-VS-TR-2003-1547

11. SUPPLEMENTARY NOTES

12 a. DISTRIBUTION / AVAILABILITY STATEMENT

Approved for public release, distribution unlimited

12 b. DISTRIBUTION CODE

13. ABSTRACT (Maximum 200 words)

This document is a report of the technical progress made during the period 01 Aug. 2001 - 31 July 2002 in the areas of: (1) research, evaluation and adaptation of particle transport simulation programs for modeling the detection and measurement of space radiation by space-borne sensors; (2) construction of realistic flight sensor computer models; (3) performance of particle transport calculations; (4) space-borne dosimeter simulation studies; (5) studies of scattering of grazing incidence protons from surfaces of material constituents of space-borne X-ray telescopes. The computer programs ITS/ACCEPT and MCNPX were applied to the modeling of the CEASE and HEP sensors. Shown in this report are listings of input and output files, with geometry/materials drawings, for the various simulation programs, annotated computer code listings showing program modifications, and partial listings of computer code outputs.

14. SUBJECT TERMS Electron and proton transport; Monte Carlo simulation; Space-borne sensor modeling; ITS/ACCEPT Code; MCNPX Code; Dosimeters; grazing angle proton scatter

15. NUMBER OF PAGES

58

16. PRICE CODE

17. SECURITY CLASSIFICATION OF REPORT

UNCLASSIFIED

18. SECURITY CLASSIFICATION OF THIS PAGE

UNCLASSIFIED

19. SECURITY CLASSIFICATION OF ABSTRACT

UNCLASSIFIED

20. LIMITATION OF ABSTRACT

SAR



## Contents

	Page
1. Introduction	1
2. Electron Transport Modeling	1
2.1 CRRES Dosimeter Models – MCNPX and ITS/ACCEPT	1
2.1.1 CRRES_D1 MCNPX Calculations	5
2.1.2 CRRES_D1 ITS/ACCEPT Calculations	7
2.2 HEP- Electron Transport Modeling	12
3. Proton Transport	12
3.1 CEASE – MCNPX Proton Transport Modeling	12
3.2 Grazing Angle Proton Scattering Calculations	12
4. Summary	21
5. References	21
Appendix 1	
Subroutine HIST for Cosine-Weighted Dome Source	21
Appendix 2	
CRRES_D1 Sample Input File for ACCEPT Run	29
Appendix 3	
CEASE Telescope - MCNPX Flat Disk Proton Source Runs	33
Appendix 4	
MCNPX Output File for Grazing Angle Proton Scattering Study 250 keV Proton Beam Incident on Iridium Slab, Angle of Incidence = $0.1^\circ$	39
Appendix 5	
MCNPX Source Subroutine for Grazing Angle Proton Scattering Study	47
Appendix 6	
PHILOOK, Program for Extraction and Conversion to Histogram Form of Emergent Proton Azimuthal Distributions from MCNPX PTRAC File Output Produced in the Grazing Angle Proton Scattering Study	49

## List of Figures

	Page
Figure 1. CRRES_D1 Dosimeter run file, LANL Version for MCNP.	2
Figure 2. CRRES_D2 Dosimeter run file, LANL Version for MCNP.	3
Figure 3. VISED rendering of MCNP cell geometry configuration for CRRES_D1, corresponding to the listing shown in Figure 1.	4
Figure 4. VISED rendering of MCNP surface geometry configuration for CRRES_D1, corresponding to the listing shown in Figure 1.	4
Figure 5. Angular orientation diagram for cosine-weighted source incident on CRRES dosimeter dome at $(x_o, y_o, z_o)$ . $\Theta$ is the angle of rotation about the $x$ -axis. $\theta'$ is the polar angle between the source electron direction and the $z'$ axis.	8
Figure 6. Comparison of Flux and Dose Response functions calculated with ITS/ACCEPT and as reported in [1].	10
Figure 7. Problem geometry – proton beam incident on material slab.	12
Figure 8. Sample plots of probability density $P_{E_{in}}((\theta_{out} - 90^\circ)/(\theta_{in} - 90^\circ); E_{out})$ of emergent protons with exit polar angle $\theta_{out}$ , for incident angle $\theta_{in} = 90.5^\circ$ , for source energy $E_{in} = 250$ keV and exit energy bins $E_{out} = 0-12.5, 12.5-25.0, 25.0-37.5, 37.5-50.0, 50.0-62.5$ keV.	15
Figure 9. Emergent proton pulse-height distribution $N(E_{out}, \theta_{out}; E_{in}, \theta_{in})$ for 250 keV protons incident on Iridium slab at $\theta_{in} = 91.0^\circ$ . Results are shown for $0 \leq \theta_{out} < 85^\circ$ in $5^\circ$ increments.	16
Figure 10. Emergent proton pulse-height distribution $N(E_{out}, \theta_{out}; E_{in}, \theta_{in})$ for 250 keV protons incident on Iridium slab at $\theta_{in} = 91.0^\circ$ . Results are shown for $85^\circ \leq \theta_{out} \leq 90^\circ$ in $0.1^\circ$ increments.	17
Figure 11. Pulse-height energy spectrum $N(E_{out}; E_{in}, \theta_{in})$ for protons emerging from iridium slab. $E_{in}=250$ keV, $\theta_{in}=90.5^\circ$ .	18
Figure 12. Emergent proton azimuthal ( $\varphi_{out}$ ) distribution (normalized) from protons incident on iridium slab. $\varphi_{in} = 90.0^\circ$ ; $E_{in}=500$ keV; $\theta_{in}= 91.0^\circ$ .	19
Figure 13. Maximum value of the probability density $P_{max}(E_{out}; E_{in}, \theta_{in})$ vs. $E_{out}$ for protons of energy $E_{in}=1.0$ MeV incident on iridium at $\theta_{in} = 90.1^\circ$ .	20
Figure 14. $\theta_{out}/\theta_{in} _{P_{max}}$ vs. $E_{out}$ for protons of energy $E_{in}=1.0$ MeV incident on iridium at $\theta_{in} = 90.1^\circ$ .	20

## List of Tables

	<b>Page</b>
Table 1. Energy Deposition (MeV) in CRRES_D1 Dosimeter (Cell #1, Figures 1,3)	6
Table 2. Comparison of ITS/ACCEPT and MCNPX Energy Deposition (MeV) Calculations for CRRES_D1 Dosimeter (ALL CELLS, Figures 1,3) for Four Source Energies	11





## 1. INTRODUCTION

The effort to be described in this report was performed as partial fulfillment of two primary objectives: (1) perform computer simulations of charged particle transport, energy and charge deposition in satellite-borne instrumentation used in research efforts of the Air Force Research Laboratory/Space Weather Center of Excellence (AFRL/VSBXR) to detect and characterize (by type, energy, intensity, *etc.*) particles associated with ionizing radiation in space; (2) transfer this simulation capability to AFRL/VSBXR and provide advice to Air Force researchers on its use; and (3) perform studies of transport code predictions of grazing angle proton scattering. In the following sections, we provide descriptions and examples of particle transport simulations and their application to problems of interest to AFRL/VSBXR.

## 2. ELECTRON TRANSPORT MODELING

### 2.1 CRRES Dosimeter Models – MCNPX and ITS/ACCEPT

A series of flux and dose response functions for electrons and protons were calculated by Auchampaugh and Cayton [1] for electron, secondary photon and proton transport in the CRRES (Combined Release and Radiation Effects Satellite) dosimeters. The calculations were made in 1992 using the then current versions of MCNP[2] for electron and photon transport and LAHET[3] for the proton transport. Since that time, the MCNP and LAHET codes have been superceded by MCNPX[4]. Also, our experience has shown that the electron transport calculations can in general be performed more efficiently using ITS/ACCEPT[5] rather than MCNPX. For this reason, as well as recognition of significantly (since 1992) reduced computation cost, we undertook to repeat some of the electron/photon transport calculations of [1] using both the MCNPX and ACCEPT codes, thus providing an "in-house" Air Force capability to perform these and other simulations as may be needed in the future.

The original MCNP geometry files from [1] for the CRRES\_D1, D2, D3 and D4 dosimeters were supplied by D. Brautigam (AFRL)[6]. The D1 and D2 files are shown in Figures 1 and 2, respectively.

We used the visual editor program VISED[7]for MCNP input files to assist in the interpretation of the geometry files shown in Figures 1 and 2. This visualization is shown in Figures 3 and 4, which are the diagrams for the CRRES\_D1 cell and surface configurations, respectively. VISED provides the color rendering to distinguish among the five materials specified by the "mX" (X=1-Si; 2-Al; 3-Al<sub>2</sub>O<sub>3</sub>; 4-Ni; 5-W,Fe alloy). records in the geometry files.

```

Geometry for CRRES dosimeter dome 1
-- 11 Feb 92
1 1 -2.33 11 -10 -3
2 1 -2.33 11 -10 3 23 -24 25 -26
3 0 11 -10 (-23:24:-25:26) -2
4 0 10 -2
5 2 -2.700 2 -1 10
6 2 -2.700 2 -1 11 -10
7 0 12 -11 -22
8 0 13 -12 -5
9 3 -3.700 12 -11 22 -8
10 2 -2.700 12 -11 8 -7
11 2 -2.700 13 -12 5 -7
12 4 -8.900 14 -13 -5
13 2 -2.700 14 -13 5 -7
14 2 -2.700 15 -14 -7
15 5 -18.30 17 -15 -6
16 2 -2.700 17 -15 6 -7
17 2 -2.700 17 -16 7 -9
18 0 16 -11 7 -9
19 0 11 1 -18
20 0 ((11 18):(-11 9):-17) -20
21 0 20
22 0 21

1 so 1.22936
2 so 1.01981
3 cz 0.05093
4 cz 0.76200
5 cz 0.32385
6 cz 1.11125
7 cz 1.22936
8 cz 0.50800
9 cz 1.46812
10 pz 0.04030

11 pz 0.00000
12 pz -0.07620
13 pz -0.10668
14 pz -0.15748
15 pz -0.31496
16 pz -0.94996
17 pz -1.58496
18 so 1.46812
19 so 1.32000
20 so 50.0
21 pz -0.0000001
22 cz 0.06350
23 px -0.09525
24 px 0.09525
25 py -0.09525
26 py 0.09525

mode p e
imp:p,e 1 19r 0 1
m1 14000 1.
m2 13000 1.
m3 8000 -0.47075 13000 -0.52925
m4 28000 1.
m5 74000 -0.95 26000 -0.05
sdef sur=19 ccc=22 nrm=-1. dir=d1
par=3 erg=5.0
sb1 -21 1
sp1 -21 1
f108:p,e 1
e108 0. .049 .051 .125 .193 .263 .336
.408 .480 .549 .622 .694 .765
.839 .910 0.979 1.020 1.28 1.91 2.56
3.20 3.84 4.48 5.12 5.74
6.37 7.01 7.67 8.30 8.94 9.57 10.1
41.2 104. t
phys:e 25.5

```

Figure 1. CRRES\_D1 Dosimeter run file, LANL Version[1], for MCNP[2].

```

Geometry for CRRES dosimeter dome 2
-- 11 Feb 92
1 1 -2.33 11 -10 -3
2 1 -2.33 11 -10 3 23 -24 25 -26
3 0 11 -10 (-23:24:-25:26) -2
4 0 10 -2
5 2 -2.700 2 -1 10
6 2 -2.700 2 -1 11 -10
7 0 12 -11 -22
8 0 13 -12 -5
9 3 -3.700 12 -11 22 -8
10 2 -2.700 12 -11 8 -7
11 2 -2.700 13 -12 5 -7
12 4 -8.900 14 -13 -5
13 2 -2.700 14 -13 5 -7
14 2 -2.700 15 -14 -7
15 5 -18.30 17 -15 -6
16 2 -2.700 17 -15 6 -7
17 2 -2.700 17 -16 7 -9
18 0 16 -11 7 -9
19 0 11 1 -18
20 0 ((11 18):(-11 9):-17) -20
21 0 20
22 0 21

13 pz -0.10668
14 pz -0.15748
15 pz -0.31496
16 pz -0.94996
17 pz -1.58496
18 so 1.90500
19 so 1.76000
20 so 50.0
21 pz -0.0000001
22 cz 0.12700
23 px -0.19685
24 px 0.19685
25 py -0.19685
26 py 0.19685

mode p e
imp:p,e 1 19r 0 1
m1 14000 1.
m2 13000 1.
m3 8000 -0.47075 13000 -0.52925
m4 28000 1.
m5 74000 -0.95 26000 -0.05
sdef sur=19 ccc=22 nrm=-1. dir=d1
par=3 erg=2.00
sb1 -21 1
sp1 -21 1
f108:p,e 1
e108 0. .051 .066 .134 .217 .287 .356
.434 .507 .579 .655 .735 .807
.885 .955 1.035 1.26 1.95 2.58 3.23
3.87 4.51 5.13 5.75
6.38 7.02 7.66 8.28 8.91 9.83 10.21
42.1 104. t
phys:e 5.5

1 so 1.74498
2 so 1.15443
3 cz 0.12741
4 cz 0.76200
5 cz 0.32385
6 cz 1.54813
7 cz 1.74498
8 cz 1.14300
9 cz 1.90500
10 pz 0.04340
11 pz 0.00000
12 pz -0.07620

```

Figure 2. CRRES\_D2 Dosimeter run file, LANL Version [1],for MCNP[2].

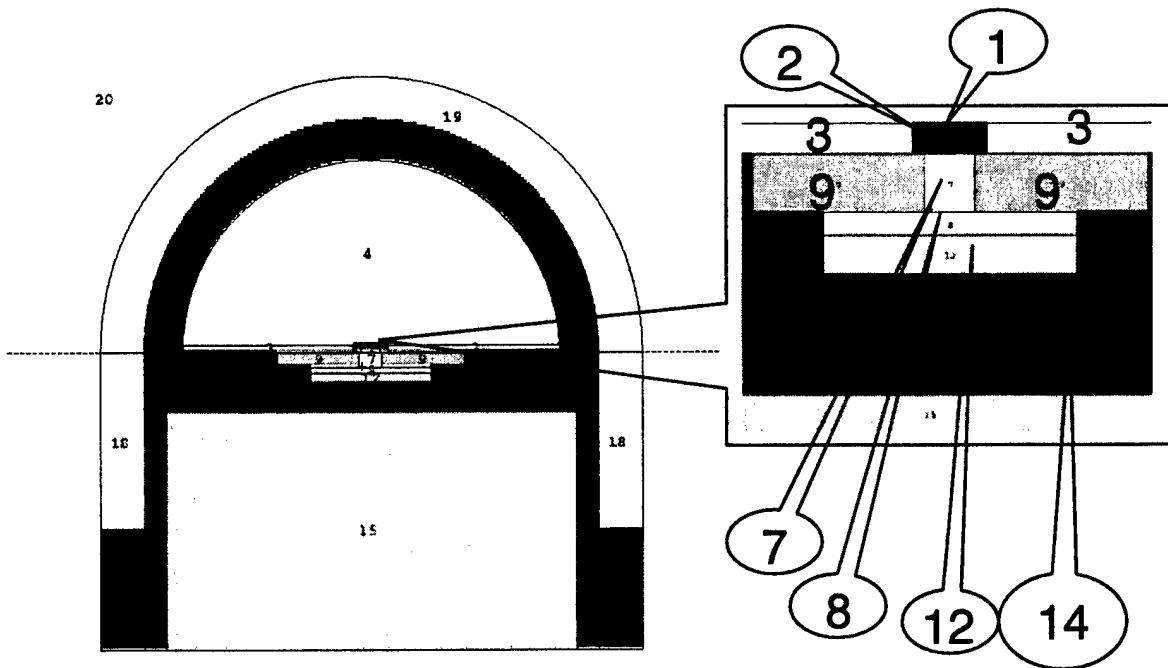


Figure 3. VISED [7] rendering of MCNP cell geometry configuration [1] for CRRES\_D1, corresponding to the listing shown in Figure 1.

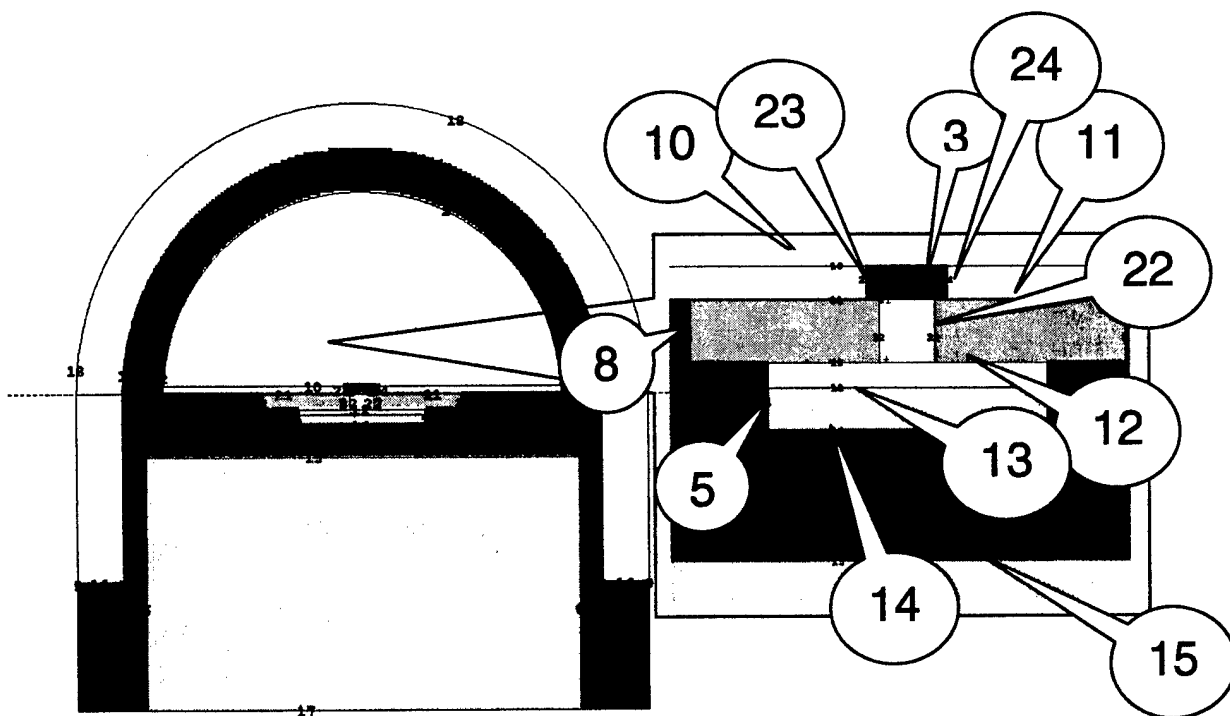


Figure 4. VISED [7] rendering of MCNP surface geometry configuration [1] for CRRES\_D1, corresponding to the listing shown in Figure 1.

### 2.1.1 CRRES\_D1 MCNPX Calculations

The authors[1] used a cosine-weighted source (as specified by the “sdef, sb1 and spl” records of Figures 1 and 2). A cosine-weighted current source corresponds to an isotropic flux of electrons incident on the dome surface. In general, the relationship between current  $j$  and flux  $\phi$  is

$$j(\mu) = \mu\phi(\mu) \quad (1)$$

where  $\mu$  is the cosine of the polar angle between the particle direction and the normal to the surface of incidence.

In the LANL calculations[1] it was assumed that the source particles originated on a hemispherical surface concentric with, but slightly larger than, the dosimeter dome. The CRRES\_D1 input file (Figure 1) was used to perform energy deposition calculations in the silicon dosimeter (cell #1 as defined in Figure 1) with MCNPX for four electron source energies, 2, 5, 10, 25 MeV, and the results were compared with those obtained in [1]. These comparisons are shown in Table 1. We computed the energy deposition using two methods: 1) the energy deposition tally supplied by MCNPX; and 2) the method used in [1], a summation over the pulse height distribution of energy deposited. The energy deposition tally capability had not yet been incorporated into MCNP when the calculations of [1] were made. Only the pulse height distribution summation method was available at that time.

Table 1. Energy Deposition (MeV) in CRRES\_D1 Dosimeter (Cell #1, Figures 1,3)

SOURCE ENERGY (MEV)	MCNPX METHOD 1 COSINE WEIGHTED	MCNPX METHOD 2 COSINE WEIGHTED	ACCEPT METHOD 1 COSINE WEIGHTED	ACCEPT METHOD 2 COSINE WEIGHTED	AUCHAM-PAUGH & CAYTON [1] <sup>1</sup>	ACCEPT METHOD 1 ISOTROPIC IN COSINE	ACCEPT METHOD 2 ISOTROPIC IN COSINE
0.2			2.232e-8	8.791e-9	5.90e-10	0	0
0.3			1.108e-8	0	1.41e-9	9.512e-9	0
0.5			2.698e-8	8.791e-9	3.81e-9	1.708e-8	8.791e-9
1			4.445e-8	2.258e-8	2.33e-7	6.560e-8	2.468e-8
1.5			6.059e-5	6.017e-5	4.27e-5	4.615e-5	4.581e-5
2	1.790e-4	1.856e-4	1.975e-4	1.984e-4	1.07e-3	1.627e-4	1.610e-4
3			3.114e-4	3.106e-4	1.86e-4	2.580e-4	2.558e-4
4			3.060e-4	3.054e-4	2.09e-4	2.477e-4	2.459e-4
5	2.898e-4	3.193e-4	2.668e-4	2.732e-4	2.56e-4	2.166e-4	2.185e-4
6			2.604e-4	2.678e-4	2.73e-4	1.951e-4	2.009e-4
7			2.454e-4	2.564e-4	2.73e-4	1.805e-4	1.861e-4
7.5			2.467e-4	2.552e-4	2.50e-4	1.829e-4	1.893e-4
10	2.828e-4	2.846e-4	2.380e-4	2.899e-4	2.69e-4	1.679e-4	1.737e-4
12.5			2.324e-4	2.415e-4	2.77e-4	1.570e-4	1.689e-4
15			2.261e-4	2.431e-4	2.73e-4	1.572e-4	1.676e-4
20			2.156e-4	2.372e-4	2.63e-4	1.523e-4	1.583e-4
25	2.729e-4	3.222e-4	2.215e-4	2.433e-4	2.60e-4	1.497e-4	1.648e-4

<sup>1</sup> Ref. 1 (Energy Deposition) /  $\Omega$

### 2.1.2 CRRES\_D1 ITS/ACCEPT Calculations

The CRRES\_D1 geometry and materials data given in Figure 1, along with the VISED diagrams for the cells and surface definitions were used to generate input data files for the ITS/ACCEPT coupled electron/photon Monte Carlo program. The cosine-weighted current source is a standard source option in the ITS/ACCEPT program. It is implemented by sampling the incident polar cosine of the source particle as follows:

With  $\mu$  defined as in Eq. 1 (above), then

$$\mu = \sqrt{\xi} \quad (2)$$

where  $\xi$  is a pseudo-random number uniformly distributed between 0 and 1. This is equivalent to sampling

$$\mu^2 = \xi \quad (3)$$

which then corresponds to the weighting of the sampled cosine,  $\mu$ , by  $\mu$  itself. It can be readily shown that for the weighting function  $f(\mu) \equiv \mu$  the cosine-weighted source has, for a negatively or inward-directed normal, an average cosine given by

$$\langle \mu \rangle = \frac{\int_{-1}^0 \mu f(\mu) d\mu}{\int_{-1}^0 f(\mu) d\mu} = -\frac{2}{3}, \quad (4)$$

and an average incident polar angle given by

$$\langle \theta \rangle = \frac{\int_{-1}^0 \cos^{-1} \mu f(\mu) d\mu}{\int_{-1}^0 f(\mu) d\mu} = \frac{3\pi}{4}, \quad (5)$$

a necessary condition for uniform angular distribution (isotropic flux) with respect to the normal to the surface of impingence.

The cosine-weighted source option is coded into the original version of ITS/ACCEPT for source particles incident on a plane surface. To apply the cosine-weighted current source methodology to the dome geometry, we modified the dome source option that we had previously written for the ITS/ACCEPT code [8]. In Figure 5 we define the  $(x,y,z)$  axes to be the inertial reference frame for the standard velocity direction cosines  $(\alpha, \beta, \gamma)$  as defined in ITS/ACCEPT, *i.e.* in terms of the polar and azimuthal angles  $\theta$  and  $\phi$  of the particle trajectory,

$$\begin{aligned} \alpha &= \sin \theta \cos \phi, \\ \beta &= \sin \theta \sin \phi, \\ \gamma &= \cos \theta. \end{aligned} \quad (6)$$

The primed coordinate system is defined by a rotation through angle  $\Theta$  about the  $x$ -axis, as shown in Figure 5. The velocity direction cosines  $(\alpha', \beta', \gamma')$  of the source electron in the primed system are correspondingly

$$\begin{aligned}\alpha' &= \sin \theta' \cos \phi', \\ \beta' &= \sin \theta' \sin \phi', \\ \gamma' &= \cos \theta'.\end{aligned}\tag{7}$$

The procedure to determine the orientation, expressed in the unprimed or inertial system, of the individual source electrons is as follows:

- 1) choose the point of particle incidence  $(x_o, y_o, z_o)$  to specify the rotation angle  $\Theta$  by random uniform sampling on the hemispherical surface (Figure 5);
- 2) sample  $\cos \theta' = -\sqrt{\xi}$ , where as before,  $\xi$  is a pseudo-random number uniformly distributed between 0 and 1;
- 3) sample  $\phi'$  uniformly on the interval  $(0, 2\pi)$ ;
- 4) compute the direction cosines  $(\alpha, \beta, \gamma)$  as

$$\begin{bmatrix} \alpha \\ \beta \\ \gamma \end{bmatrix} = \begin{bmatrix} 1 & 0 & 0 \\ 0 & \cos \Theta & \sin \Theta \\ 0 & -\sin \Theta & \cos \Theta \end{bmatrix} \begin{bmatrix} \alpha' \\ \beta' \\ \gamma' \end{bmatrix}.\tag{8}$$

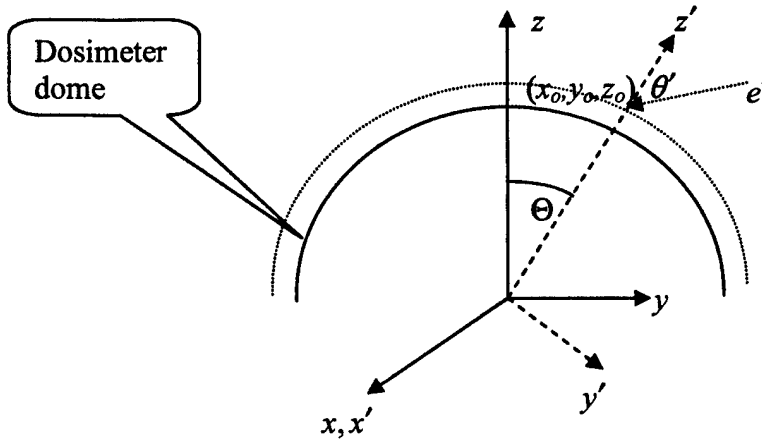


Figure 5. Angular orientation diagram for cosine-weighted source incident on CRRES dosimeter dome at  $(x_o, y_o, z_o)$ .  $\Theta$  is the angle of rotation about the  $x$ -axis.  $\theta'$  is the polar angle between the source electron direction and the  $z'$  axis.

ITS/ACCEPT was modified (subroutine HIST) to perform the above source sampling procedure. The code modifications are shown in Appendix 1.

Two sets of 17 ITS/ACCEPT runs,  $10^7$  histories each, were made for the 17 source energies (see Table 1, column 1) listed in [1]. Comparisons of our results with [1]



are shown in Table 1. In our ITS/ACCEPT and MCNPX runs, the calculations of energy deposition were made using two methods: 1) the standard method of ACCEPT and MCNPX – (energy entering cell – energy exiting cell)[Table 1, columns 2,4,7]; and 2) summation over several energy bins,  $\sum_i N(E_i)E_i$  where  $N(E_i)$  is the pulse height in energy bin  $i$  and  $E_i$  is the average energy of the bin [Table 1, columns 3,5,6,8]. This second method was employed in [1], because the direct energy deposition calculation had apparently not been installed in the MCNP version available at the time (1993).

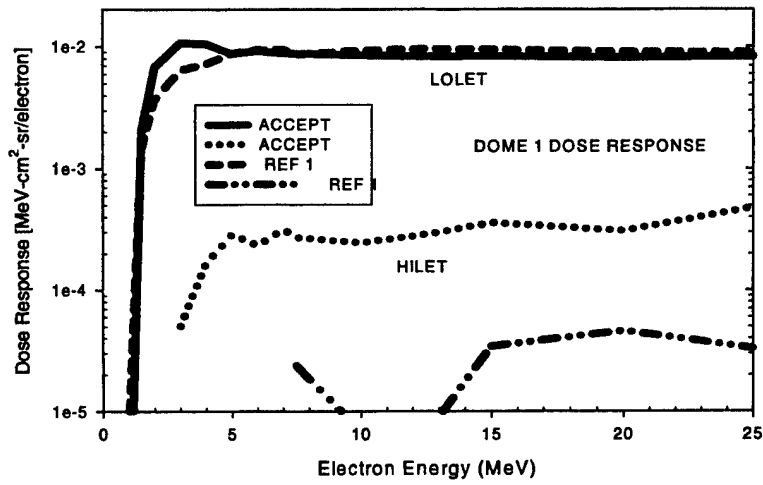
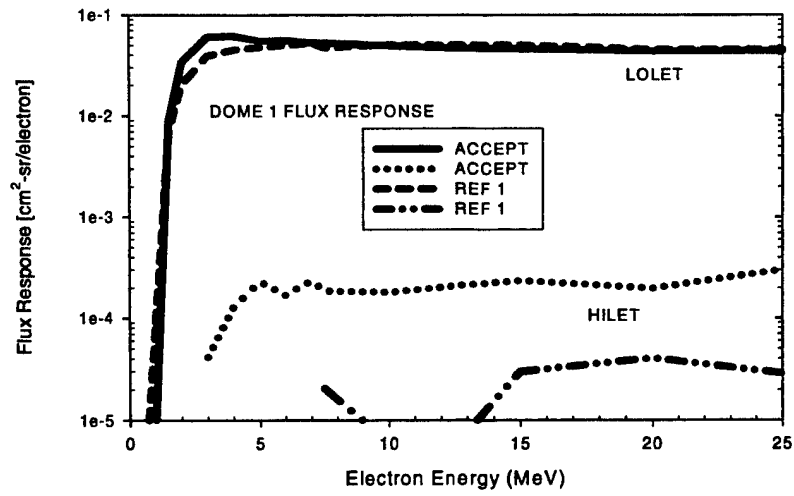
The first set of runs employed the source sampling procedure described above. A sample input file for ITS/ACCEPT is listed in Appendix 2. For comparison purposes, the runs in the second set were made for the same energies, but without cosine source weighting. The data shown in column 6 of Table 1 are the results given in [1] adjusted to correspond to the energy deposition units (MeV) produced by the ITS/ACCEPT and MCNPX calculations. In [1], the energy deposition results are given in units of MeV-cm<sup>2</sup>-steradian per source electron, with the solid angle  $\Omega$  factor for the CRRES\_D1 geometry taken as 34.39 cm<sup>2</sup>-steradian. The data of column 6 are the raw results given in [1] divided by this solid angle factor.

In Figure 6 we plot the silicon dosimeter (cell 1, Figure 3) flux response vs. source electron energy and dose response vs. source electron energy curves obtained with our calculations on the same graphs as the Ref. 1 data for comparison. The flux and dose response functions are defined as

$$\text{Flux Response} = \Omega \sum_i N(E_i), \quad \text{Dose Response} = \Omega \sum_i E_i N(E_i),$$

with their respective units of cm<sup>2</sup>-steradian and MeV-cm<sup>2</sup>-steradian per source electron. The designations LOLET and HILET refer to the contributions to the response functions from electrons with energy below and above 1 MeV in the dosimeter (cell 1, Figure3), respectively.

Table 2 shows a comparison of ITS/ACCEPT and MCNPX energy deposition results in all cells (Figure 3) for the four source energies (2, 5, 10, 25 MeV) for which both programs were run.



REF 1 - Auchampaugh & Gavton

Figure 6. Comparison of Flux and Dose Response functions calculated with ITS/ACCEPT[5] and as reported in [1].

Table 2. Comparison of ITS/ACCEPT and MCNPX Energy Deposition (MeV) Calculations for CRRES\_D1 Dosimeter (ALL CELLS, Figures 1,3) for Four Source Energies.

MCNPX CELL # (FIGURE 3)	SOURCE ENERGY = 2 MEV		SOURCE ENERGY = 5 MEV		SOURCE ENERGY = 10 MEV		SOURCE ENERGY = 25 MEV	
	ACCEPT	MCNPX	ACCEPT	MCNPX	ACCEPT	MCNPX	ACCEPT	MCNPX
1	1.975E-04	1.790E-04	2.668E-04	2.898E-04	2.380E-04	2.828E-04	2.215E-04	2.729E-04
2	6.491E-04	6.471E-04	9.164E-04	1.033E-03	7.997E-04	9.973E-04	7.458E-04	9.013E-04
5+6	1.308E+00	1.225E+00	1.875E+00	1.687E+00	2.124E+00	1.836E+00	2.205E+00	1.862E+00
10	6.332E-02	1.054E-01	1.908E-01	2.311E-01	1.943E-01	2.447E-01	1.732E-01	2.360E-01
9	4.008E-02	3.273E-02	8.126E-02	7.564E-02	6.787E-02	7.610E-02	6.147E-02	7.020E-02
11	1.204E-02	2.445E-02	8.851E-02	9.467E-02	8.759E-02	1.057E-01	7.540E-02	1.029E-01
17	6.120E-06	9.523E-03	2.737E-03	1.738E-02	1.665E-02	3.348E-02	1.342E-02	5.948E-02
16	4.050E-05	5.399E-03	1.559E-02	3.233E-02	6.323E-02	7.084E-02	1.204E-01	1.209E-01
15	3.602E-03	5.721E-03	2.902E-01	3.011E-01	1.530E+00	1.397E+00	4.161E+00	4.130E+00
12	2.292E-03	2.124E-03	4.812E-02	3.726E-02	3.963E-02	4.343E-02	3.353E-02	4.116E-02
13	7.183E-03	2.261E-02	1.440E-01	1.457E-01	1.450E-01	1.662E-01	1.216E-01	1.622E-01
14	1.394E-03	2.126E-02	4.484E-01	4.224E-01	4.907E-01	5.142E-01	3.895E-01	4.866E-01
TOTAL	1.439E+00	1.455E+00	3.186E+00	3.046E+00	4.760E+00	4.488E+00	7.355E+00	7.273E+00

## 2.2 HEP- Electron Transport Modeling

Extensive testing was performed on the ITS/ACCEPT input file written[9] for the HEP instrument. This file contains a complete, blueprint matching, geometry description for the in-flight model. It was felt that, due to the complicated geometry structure of the model, it would be advisable to run an extensive series of Monte Carlo calculations for model validation. To that end four sets, each consisting of ten source positions, of (50000 history) electron transport runs were made. The first of these consisted of pencil beam, 15 MeV, sources normally incident on the “top” ( $x = 5.0$  cm) at ten uniformly distributed positions along  $z$ . The second and third sets were similarly distributed along  $z$  but were positioned on the side ( $y = 4.0$  cm) and bottom ( $x = -3.0$  cm). The fourth set consisted of calculations made with a 6-component energy (max. energy = 20 MeV) spectrum, point isotropic source embedded at ten uniformly spaced positions along the central ( $z$ ) axis. In all cases run, there were no “lost particles” attributable to geometry specification errors.

## 3. PROTON TRANSPORT

### 3.1 CEASE – MCNPX Proton Transport Modeling

Two proton transport runs were made with the CEASE telescope model [10] for MCNPX, as requested by the Air Force sponsor, for 9 MeV proton flat disk sources, located at  $z = 0.457$  cm on the telescope axis, at 40 degree slant incidence with respect to the  $z$ -axis. Partial listings of the run outputs are shown in Appendix 3. The geometry portions of these files, previously listed in [11] were omitted for brevity.

### 3.2 Grazing Angle Proton Scattering Calculations

An extensive series of proton transport calculations were made using MCNPX for protons beams incident on aluminum and iridium ( $6 \times 5 \times 1$  cm) at shallow (grazing) angles of incidence ( $\theta_{in} = 90.1, 90.5, 91.0^\circ$ ,  $\phi = 90.0^\circ$  as shown in Figure 7).

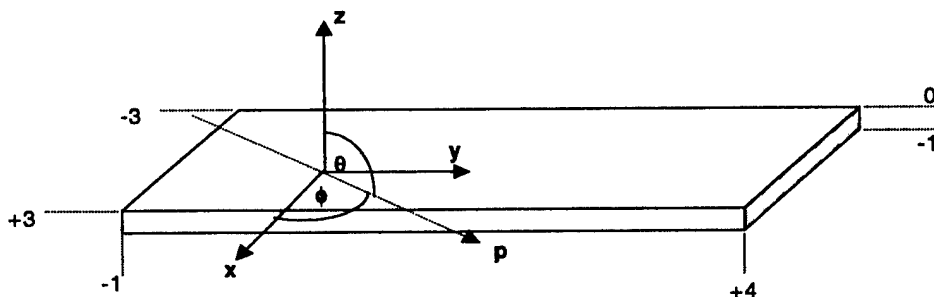


Figure 7. Problem geometry – proton beam incident on material slab

The motivation for this work was an investigation into the occurrence of unexpected radiation damage to one of the Chandra X-Ray Telescope cameras by grazing incidence protons. Standard Monte Carlo codes, such as Geant4[12], the program used to predict radiation damage in the Chandra, produced erroneous results. In our calculations we set out to investigate the treatment by standard Monte Carlo programs such as MCNPX of

the energy loss and relationship between the beam angle of incidence and the emergent angular distribution (from the top surface or vacuum interface of a material medium) for protons with grazing incident angles. To accomplish this, we ran MCNPX for 0.25 MeV protons incident on aluminum and 0.05, 0.25, 0.5, 1.0 MeV protons incident on iridium slabs at grazing angles. All of the Monte Carlo calculations were made using  $10^8$  case histories to ensure statistical reliability. High angular resolution emergent proton spectra were obtained, and plots made, for energy-angle, total energy, and azimuthal distributions.

The MCNPX proton transport results were analyzed from several aspects. Programs were written to convert the raw Monte Carlo data to histograms detailing:

- (1) probability density  $P_{E_{in}} \left( \frac{(\theta_{out} - 90^\circ)}{(\theta_{in} - 90^\circ)}; E_{out} \right)$  of emergent protons with exit polar angle  $\theta_{out}$ , for every fixed incident angle  $\theta_{in}$ , for every source energy  $E_{in}$  and exit energy bin width  $\Delta E_{out} = 0.05 E_{in}$ . Representative plots of the probability density function for 0.25 MeV ( $=E_{in}$ ) protons incident on iridium with incident angle 90.5 degrees ( $=\theta_{in}$ ), are shown in Figure 8. The five plots represent the emergent proton probability densities for the five emergent energy intervals 0-12.5, 12.5-25.0, 25.0-37.5, 37.5-50.0, 50.0-62.5 keV.
- (2) emergent proton pulse-height distribution histogram plots  $N(E_{out}, \theta_{out}; E_{in}, \theta_{in})$ ; Representative plots are shown in Figures 9 and 10 for 0.25 MeV ( $=E_{in}$ ) protons incident on iridium with incident angle 91.0 degrees ( $=\theta_{in}$ ). The emergent proton pulse-height distributions were calculated using 5 degree coarse resolution emergent angle ( $\theta_{out}$ ) bins in the range  $0 \leq \theta_{out} < 85^\circ$  (Figure 9) and 0.1 degree high resolution bins in the range  $85^\circ \leq \theta_{out} \leq 90^\circ$  (Figure 10). The pulse-height distributions, expressed as the number of emergent protons per energy-angle bin, per incident proton, are normalized to unit proton incidence.
- (3) emergent proton pulse-height energy spectra  $N(E_{out}; E_{in}, \theta_{in})$   $[= \sum_{\theta_{out}} N(E_{out}, \theta_{out}; E_{in}, \theta_{in})]$ . The plot shown in Figure 11 is the pulse-height energy spectrum of emergent protons resulting from a 0.25 MeV proton beam incident on iridium with angle 91.0 degrees ( $=\theta_{in}$ ).
- (4) emergent proton azimuthal ( $\phi_{out}$ ) distribution. The plot shown in Figure 12 is the distribution of  $\phi_{out}$  for 0.5 MeV protons incident on iridium with  $\theta_{in} = 91.0$  degrees. The emergent azimuthal distribution is strongly peaked in the incident azimuthal direction,  $\phi_{in} = 90.0$  degrees. This was found to be true for all 15 cases studied.

Additionally, plots were made for each incident energy-angle combination, of the maximum value of the probability density  $P_{\max}(E_{out}; E_{in}, \theta_{in})$  (Figure 13) and its corresponding  $\left. \frac{\theta_{out}}{\theta_{in}} \right|_{P_{\max}}$  ratio vs.  $E_{out}$  (Figure 14).

The results obtained with the MCNPX model do not exhibit specular, or near-specular, reflection[13] as may have been expected from experimental results [14,15]. Preliminary conclusions also reveal that the computed proton energy loss resulting from scatter of grazing incidence protons is an overestimation and are significantly larger than experimental observation [14,15]. In MCNPX and Geant4, proton energy loss calculations in the energy range studied are based on the assumption that the continuous slowing-down approximation applied in conjunction with the bulk material stopping power is appropriate. Pfandzelter *et al.*[15] have derived, from a study of the physics of surface potentials, expressions for the effective stopping power that applies in this situation.

Sample MCNPX output is shown in Appendix 4 for a 250 keV proton beam incident on iridium at  $0.1^\circ$  ( $\theta_{in} = 90.1^\circ$  as shown in Figure 7). The energy and angular bin structures of output emergent proton current tallies shown are as defined in items 1-3, above. For these investigations, a specialized source subroutine, listed in Appendix 5, was written for MCNPX. The azimuthal ( $\phi_{out}$ ) distribution of the emergent proton current was extracted from PTRAC files produced in the MCNPX runs. A program (PHILOOK) was written to extract the azimuthal distribution data and convert them to the histogram form exemplified by the polar plot of Figure 12.

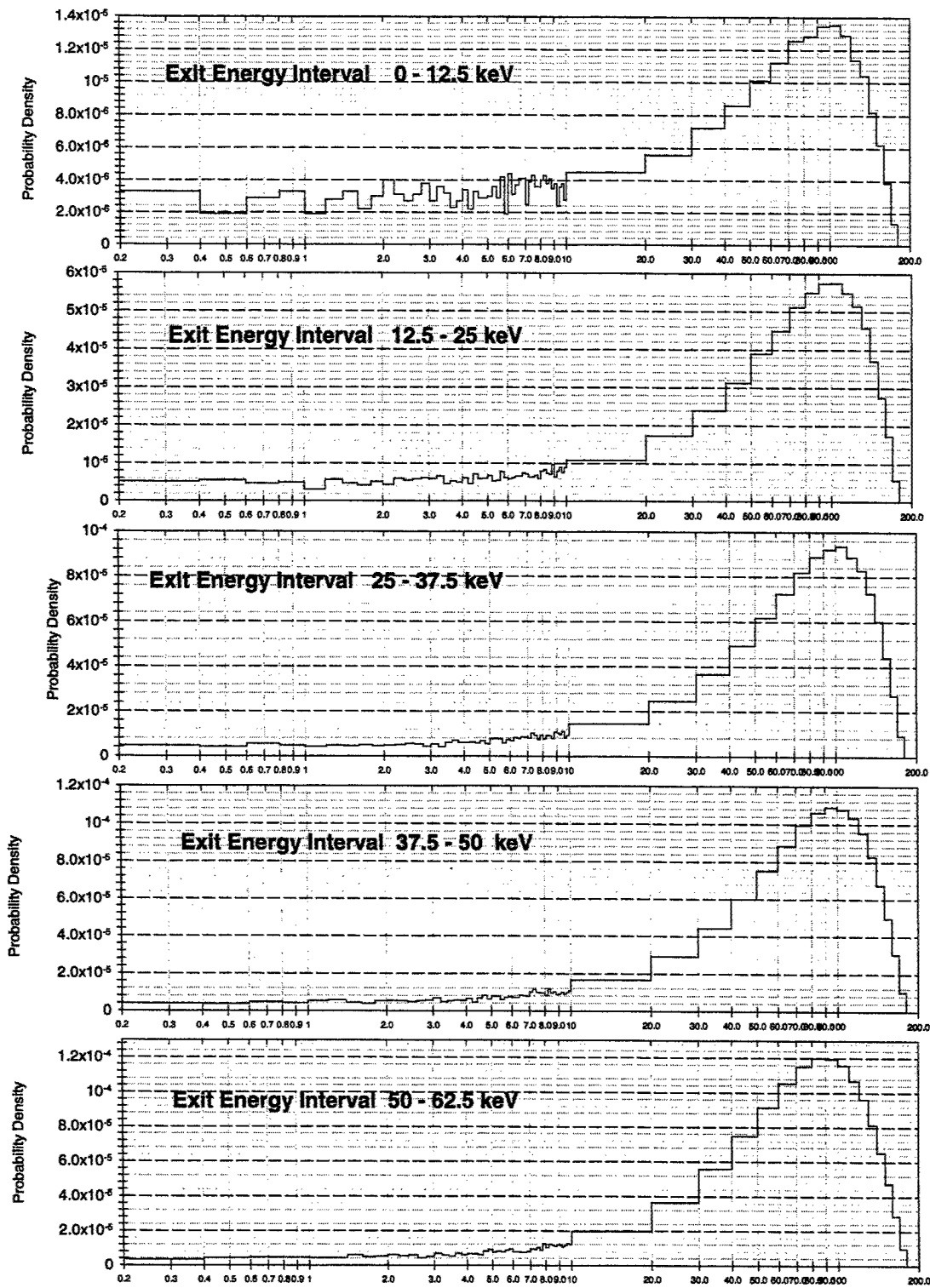


Figure 8. Sample plots of probability density  $P_{E_{in}} \left( \frac{(\theta_{out} - 90^\circ)}{(\theta_{in} - 90^\circ)}; E_{out} \right)$  of emergent protons with exit polar angle  $\theta_{out}$ , for incident angle  $\theta_{in} = 90.5^\circ$ , for source energy  $E_{in} = 250$  keV and exit energy bins  $E_{out} = 0-12.5, 12.5-25.0, 25.0-37.5, 37.5-50.0, 50.0-62.5$  keV.

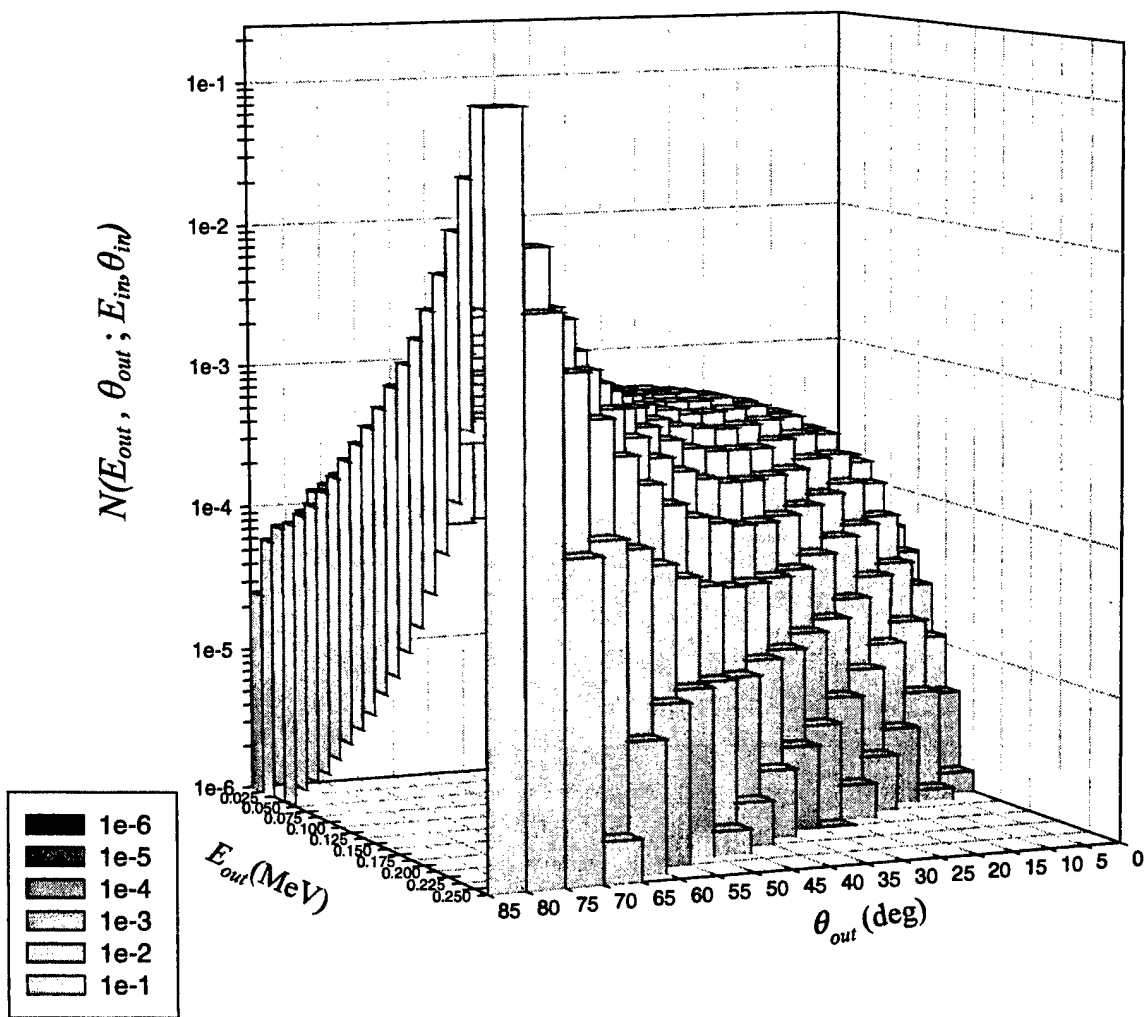


Figure 9. Emergent proton pulse-height distribution  $N(E_{out}, \theta_{out}; E_{in}, \theta_{in})$  for 250 keV protons incident on Iridium slab at  $\theta_{in} = 91.0^\circ$ . Results are shown for  $0 \leq \theta_{out} < 85^\circ$  in  $5^\circ$  increments.



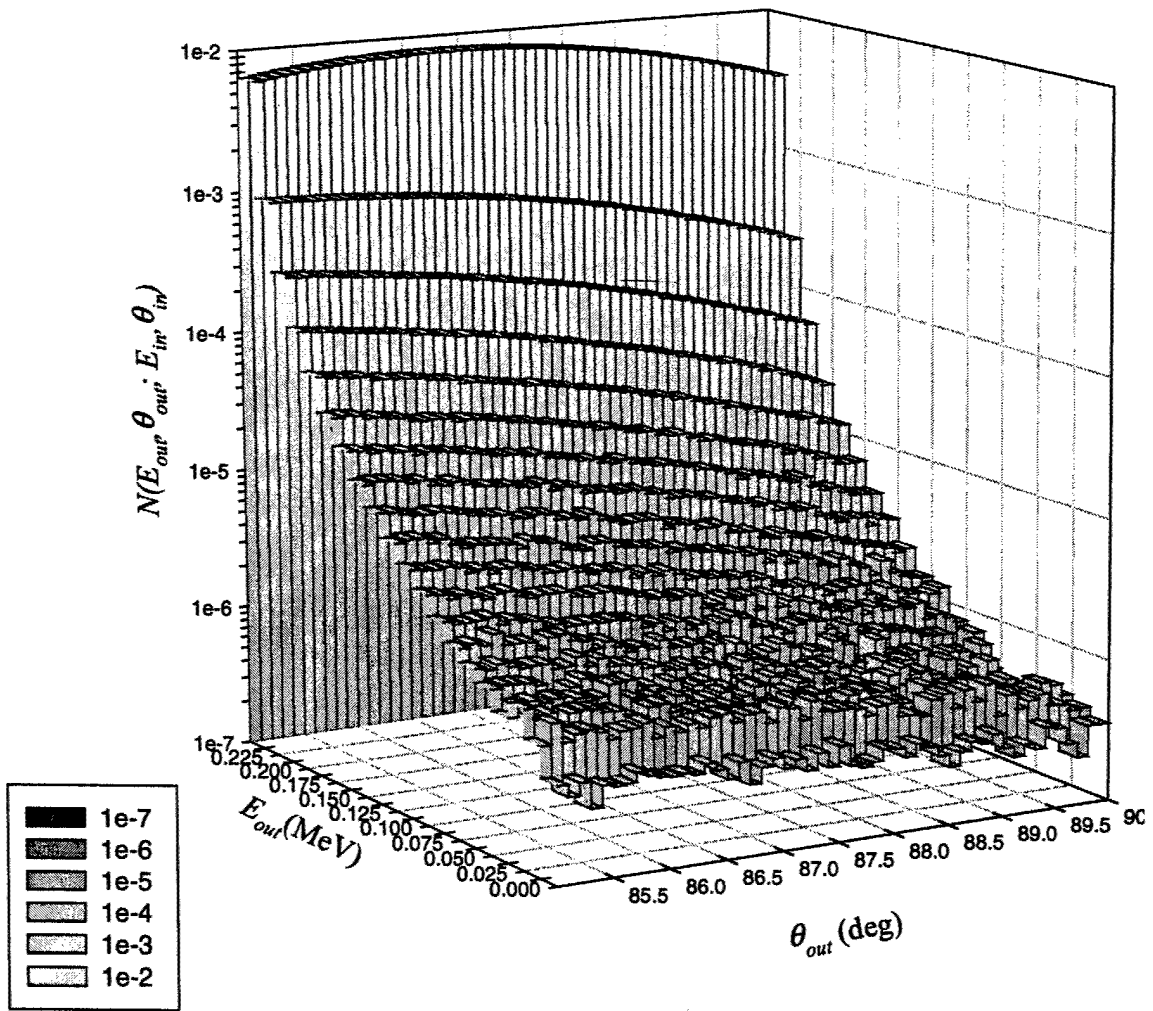


Figure 10. Emergent proton pulse-height distribution  $N(E_{out}, \theta_{out}; E_{in}, \theta_{in})$  for 250 keV protons incident on Iridium slab at  $\theta_{in} = 91.0^\circ$ . Results are shown for  $85^\circ \leq \theta_{out} \leq 90^\circ$  in  $0.1^\circ$  increments.

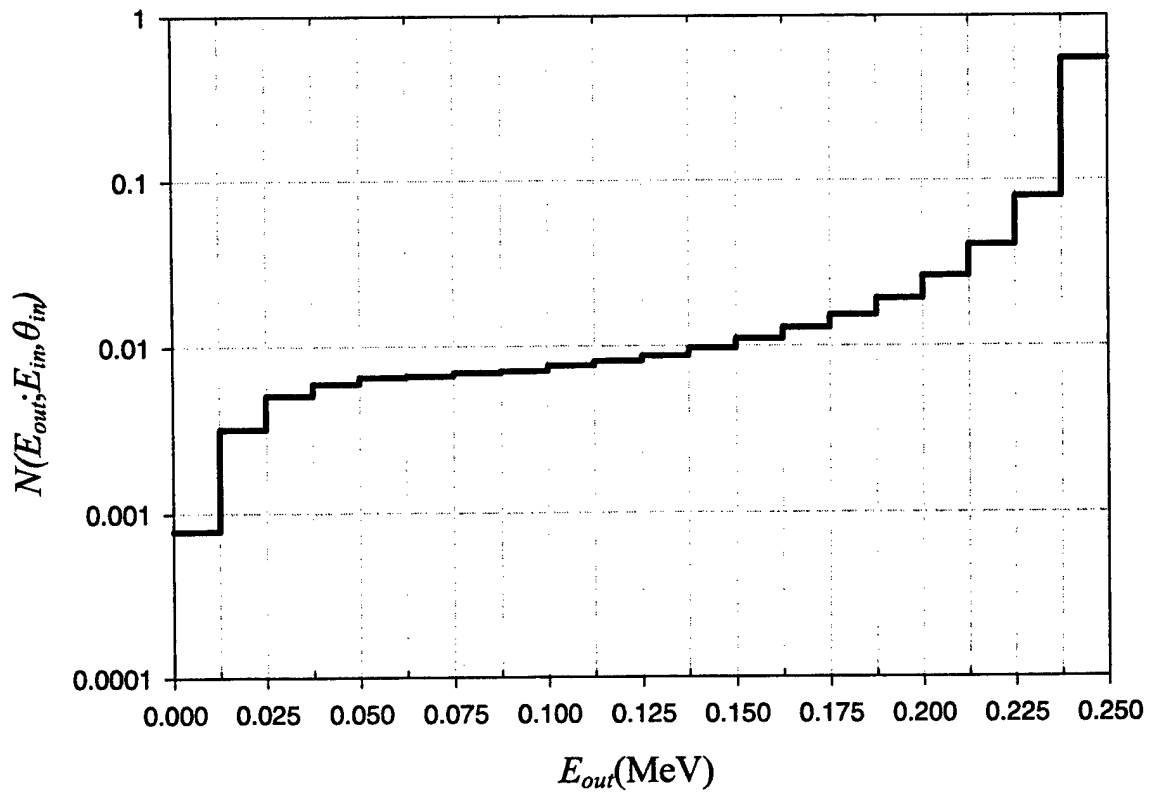


Figure 11. Pulse-height energy spectrum  $N(E_{out}; E_{in}, \theta_{in})$  for protons emerging from iridium slab.  $E_{in}=250$  keV,  $\theta_{in}=90.5^\circ$ .

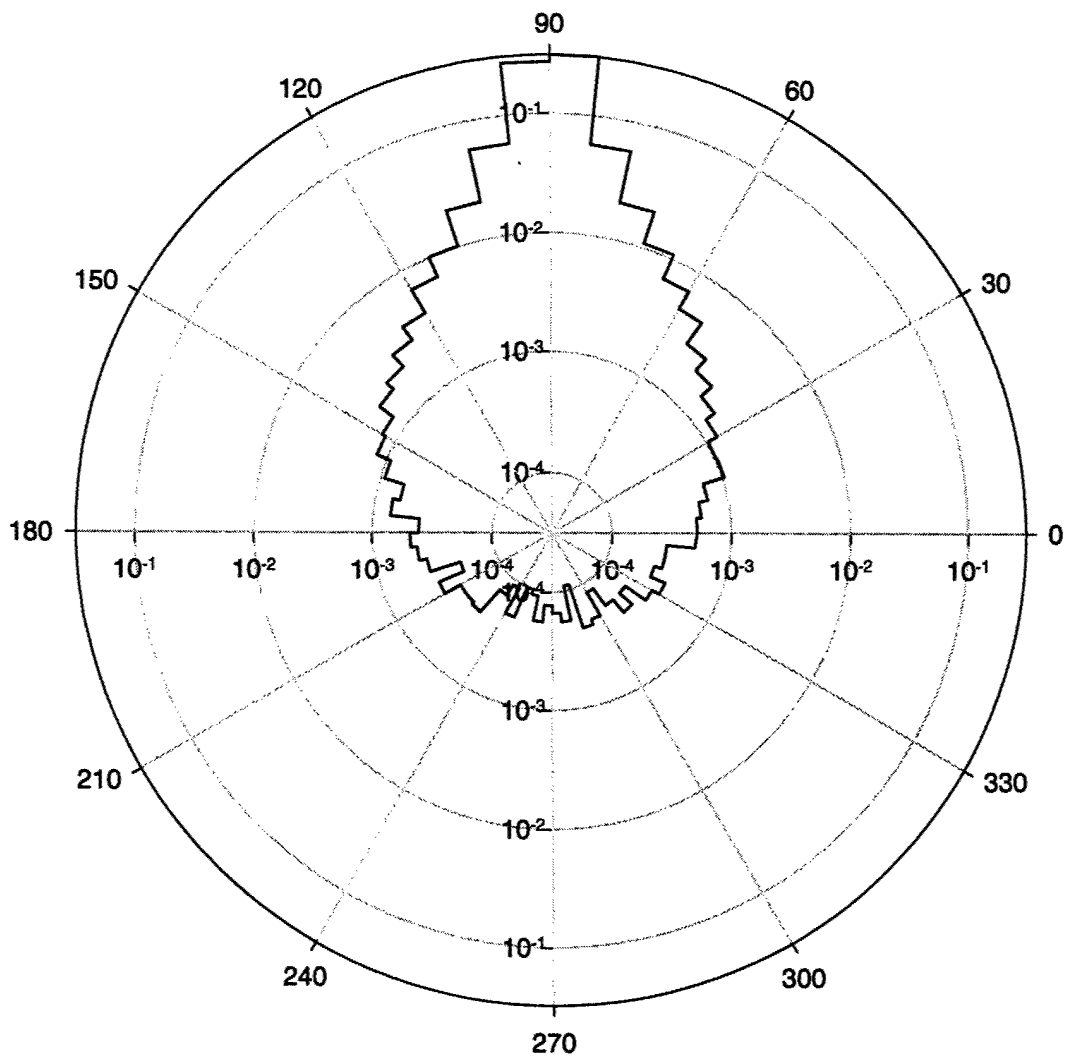


Figure 12. Emergent proton azimuthal ( $\varphi_{out}$ ) distribution (normalized) from protons incident on iridium slab.  $\varphi_{in} = 90.0^\circ$ ;  $E_{in} = 500$  keV;  $\theta_{in} = 91.0^\circ$ .

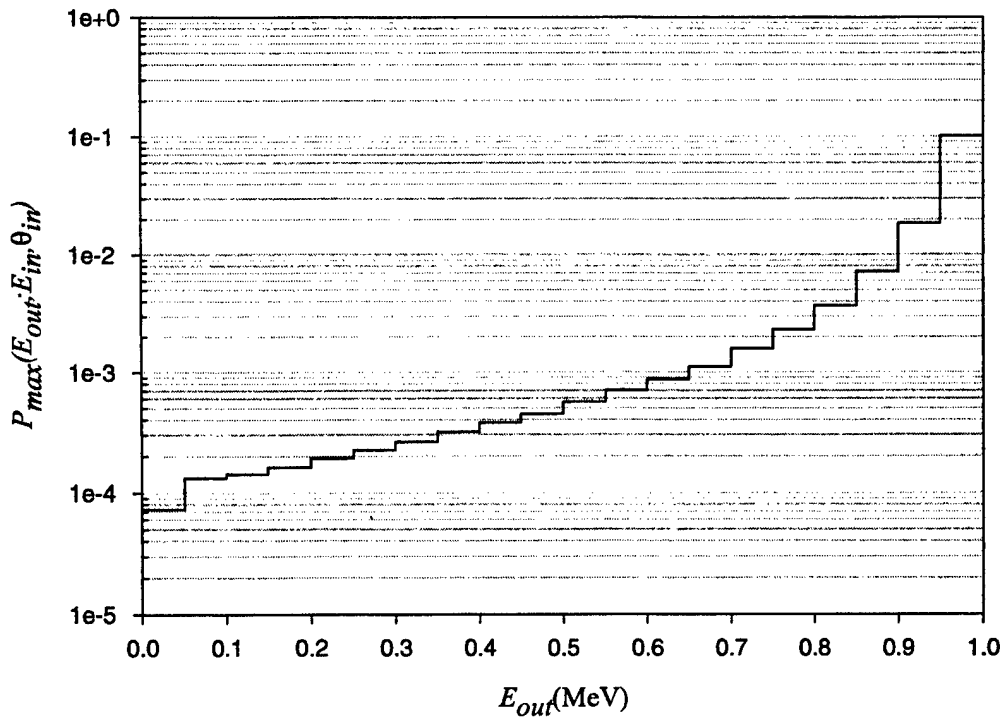


Figure 13. Maximum value of the probability density  $P_{max}(E_{out}; E_{in}, \theta_{in})$  vs.  $E_{out}$  for protons of energy  $E_{in}=1.0$  MeV incident on iridium at  $\theta_{in} = 90.1^\circ$ .

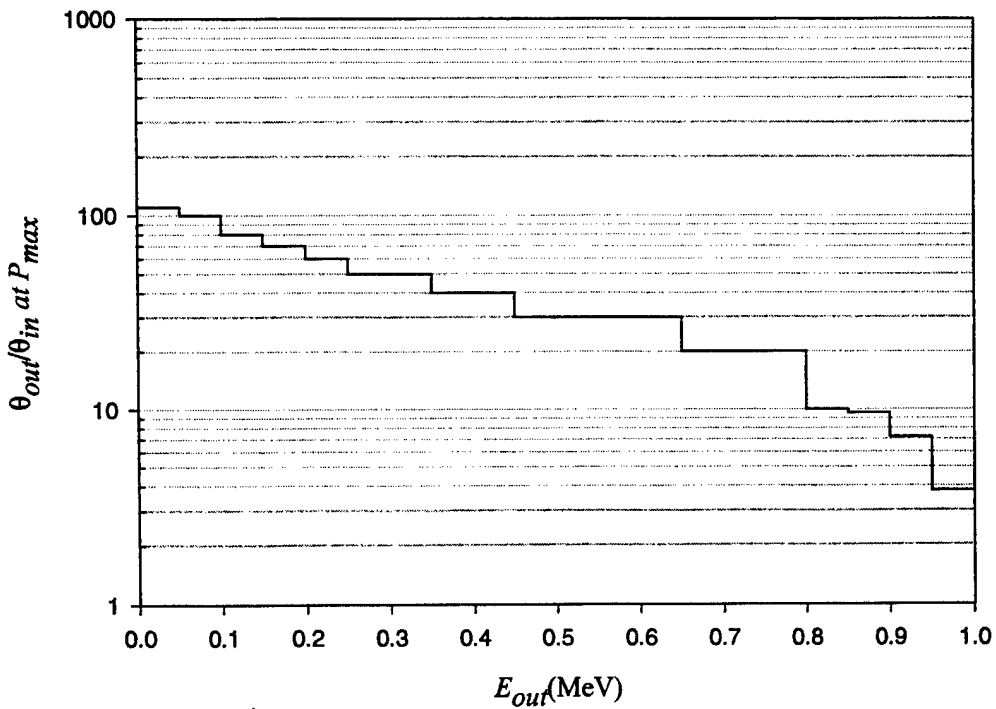


Figure 14.  $\left. \frac{\theta_{out}}{\theta_{in}} \right|_{P_{max}}$  vs.  $E_{out}$  for protons of energy  $E_{in}=1.0$  MeV incident on iridium at  $\theta_{in} = 90.1^\circ$ .

#### 4. SUMMARY

During the period covered by this report, the technical activity and progress achieved consisted primarily of: 1) modeling and verification of earlier calculations of electron transport and energy deposition in CRRES dosimeters; 2) model validation of electron transport simulations in the HEP instrument; 3) modeling proton transport in the CEASE instrument; 4) the beginning of a study of the scattering of grazing incidence protons from material surfaces; and 5) providing computer code enhancements and advice on Monte Carlo simulation code implementation to AFRL.



## References

1. Auchampaugh, G., Cayton, T., April 1993, *CRRES Dosimeter Simulations*, Los Alamos National Laboratory Report No. LA-12511-MS.
2. Briesmeister, J. F., Ed., September 1986, *MCNP – A General Monte Carlo Code for Neutron and Photon Transport*, Los Alamos National Laboratory Report LA-7396-M, Rev. 2.
3. Prael, R. E., Lichtenstein, H., September 1989, *User Guide to LCS: The LAHET Code System*, Los Alamos National Laboratory Report LA-UR-89-3014.
4. Waters, L. S., Ed., November 14, 1999, *MCNPX™, Version 2.1.5 User's Manual*, Los Alamos Radiation Transport Group(X-6).
5. Halbleib, J. A. et al., *ITS - Integrated TIGER Series of Coupled Electron /Photon Monte Carlo Code System*, ORNL RSICC Computer Code Package CCC-467.
6. Brautigam, D., May 15, 2002, AFRL/VSBXR, private communication.
7. Carter, L. L., Schwarz, R. A. *MCNP-UISED 26f - A Visual Editor for Creating MCNP4 Input Files*, ORNL RSICC Computer Code Package PSR-358.
8. Woolf, S., January 3, 2002, *Installation and Operation of Particle Transport Simulation Programs to Model the Detection and Measurement of Space Radiation by Space-borne Sensors*, ARCON Corp. Interim Scientific Report #2 (01 Aug. 2000 – 31 July 2001), Chapter 4, AFRL Contract #F19628-99-C-0077 (AD # not yet assigned).
9. Woolf, S., January 3, 2002, *Installation and Operation of Particle Transport Simulation Programs to Model the Detection and Measurement of Space Radiation by Space-borne Sensors*, ARCON Corp. Interim Scientific Report #2 (01 Aug. 2000 – 31 July 2001), Appendix 1, AFRL Contract #F19628-99-C-0077 (AD # not yet assigned).
10. B. Dichter, et al., Compact Environmental Anomaly Sensor (CEASE): A Novel Spacecraft Instrument for *In Situ* Measurements of Environmental Conditions, *IEEE Trans. Nucl. Sci.* **45(6)**, 2758, Dec. 1998.
11. Woolf, S., December 29, 2000, *Installation and Operation of Particle Transport Simulation Programs to Model the Detection and Measurement of Space Radiation by Space-borne Sensors*, Air Force Research Laboratory Report, Appendix 3, AFRL-VS-TR-2001-1605, AD # 398366.
12. Geant4 Collaboration [Online]. <http://wwwinfo.cern.ch/asd/geant4/geant4.html>
13. Firsov, O. B., 1967, *Reflection of fast ions from a dense medium at glancing angle*, *Sov. Phys.- Doklady*, vol. 11, No. 8, pp.732-733.
14. Winter, H., Wilke, M., Bergomaz, M., 1997, *Energy loss of fast protons in grazing scattering from an Al(111)-surface*, *NIM B125*, pp.124-127.
15. Pfanzelter, R., Stolzle, F., 1992, *Probing the stopping power near the surface by specular reflection of protons from graphite*, *NIM B72*, pp.163-175.

## APPENDIX 1

### Subroutine HIST for Cosine-Weighted Dome Source

```

SUBROUTINE HIST                                HIST    00007
*****                                        HIST    00009
SUBROUTINE HIST IS CALLED BY                    HIST    00010
                                           ITS      HIST    00011
SUBROUTINE HIST CALLS                          HIST    00012
  INTRINSIC FUNCTIONS                           HIST    00013
                                           SQRT, RANF  HIST    00014
                                           REAL      HIST    00015
                                           (CYLTRAN) HIST    00016
EXTERNAL FUNCTIONS                              HIST    00017
                                           CLASS, ECROS, EHIST, TIMER, PHIST HIST    00018
                                           RANINT, RANSAV  HIST    00019
                                           ZONE        HIST    00020
                                           (CYLTRAN)
                                           FOLD, ZONEA   HIST    00021
                                           (ACCEPT)
                                           PLTDAT      HIST    00022
                                           (M-CODES)
ORIGINATION DATE    16 JAN 68.                  HIST    00023
LAST MODIFIED      30 MAY 91                    HIST    00024
                                           HIST    00025
                                           HIST    00026
FUNCTION                                                    HIST    00027
  THIS PROGRAM SAMPLES PHASE SPACE PARAMETERS FOR          HIST    00028
  SOURCE PARTICLES.  SUBSEQUENTLY CALLS EITHER EHIST OR   HIST    00029
  PHIST.  RETRIEVES "BANKED" ELECTRONS AND CALLS EHIST.  HIST    00030
  TALLIES PULSE HEIGHT DISTRIBUTION.                      HIST    00031
*****                                                    HIST    00032
*** COMMON BLOCKS CNSTNT, PARAMS, OUT, CALC, XPED, STOR, STTS,
      (PAREM)-ACCEPT                                       HIST    00033
C$ LIST(S=0)                                               HIST    00034
CDIR$ NOLIST                                               HIST    00035
IMPLICIT DOUBLE PRECISION (A-H,O-Z)                       HIST    00036
SAVE                                                        HIST    00037
                                                         CNSTNT  00081
                                                         CNSTNT  00082

```

```

C
PARAMETER (CT1M12 = 1.0D-12, CT1EM8 = 1.0D-8, CT1EM7 = 1.0D-7) CNSTNT  00083
                                                         CNSTNT  00084

```

**CNSTNT common block is identical to that given in Reference 3  
– listing omitted for brevity.**

```

C
PARAMETER (CCOHLM=57.031547D0, CCOHMX=80.654788D0)          CNSTNT  00140
                                                         PARAMS  00002
C -----                                                  PARAMS  00003

```

**PARAMS common block is identical to that given in Appendix  
2, Reference 4.**

```

C -----                                                  PARAMS  00086
PARAMETER (NLAST = 50)                                       PARAMS  00089
PARAMETER ( INUMK = 3, INGP = INMT)                          PARAMS  00103
COMMON /EXTSORC/ IRECTS, IDISKS, XLOWS, XHIGHS, YLOWS, YHIGHS, ZLOWS,
$ ZHIGHS, XCENT, YCENT, ZCENT, XCIR, YCIR, ZCIR, KPERPYZ, KPREPXZ, KPERPKY,
$ IDOME, RDOME
LOGICAL RRKILL, FLMTL                                         OUT     00002
COMMON /OUT/                                                  OUT     00003

```



1 FLMTEL(INGP)

OUT 00004

**OUT common block is identical to that given in Reference 3 - listing omitted for brevity.**

\$	FLESCP, FLNOK, FLNEL, FLBAD, FLINIT, FLGSEC	OUT	00095
C		CALC	00002
	COMMON /CALC/	CALC	00003
1			04

**CALC common block is identical to that given in Reference 3 - listing omitted for brevity.**

C		CALC	00139
C		XPED	00002
	COMMON /XPED/	XPED	00003
1	DETOUR(INMT), RHO(INMT), MT, MTP, MTP0	XPED	00010
C		XPED	00012
	LOGICAL DMPFLG, FLMC	STTS	00002
	DOUBLE PRECISION IRSAV	STTS	00010
	COMMON /STTS/ IB, NB, NSORS, IBT, BOLD, BATCH, KPUTMX, DMPFLG	STTS	00017
	\$, IHIST, IRSAV, KPUT, FLMC	STTS	00018
C		STTS	00019
C		PAREM	00002
	CHARACTER*3 OTYPE(10), OBODY	PAREM	00003
	LOGICAL FLDBG, FLDBGL	PAREM	00004
	COMMON /PAREM/	PAREM	00008
	\$ XB(3), WT(3), RIN, ROUT, PINF, DIST, IR,	PAREM	00009
	\$ FLDBG, IRPRIM, ICALL, LSURF, NBO, LRI, LRO,	PAREM	00013
	\$ KLOOP, LOOP, ITYPE, FLDBGL	PAREM	00014
	COMMON /PAREMO/ OTYPE	PAREM	00015
C		PAREM	00016
	COMMON /HITS/EDPR(10), EDNK(10), EDSC(10), EDTL(10), LHCL(10), NINDV,		
	\$ IHSTRY, COFSRC(6,25,10), COFLEGY(6,25), COFLEG(6)		

C\$	LIST(S=1)	HIST	00047
CDIR\$	LIST	HIST	00048
	COMMON /STOR/	STOR	00002
1	CTHS(NLAST), TS(NLAST), WS(NLAST), ZS(NLAST), IPRS(NLAST),	STOR	00003
2	LBS(NLAST), NTS(NLAST)	STOR	00004
\$	, XS(NLAST), YS(NLAST), STHS(NLAST),	STOR	00006
3	CPHS(NLAST), SPHS(NLAST)	STOR	00007
4	, LBCS(NLAST)	STOR	00009
C		HIST	00050
	EXTERNAL RAN	RANNUM	00003
C		HIST	00089
	CIMAX = IMAX	HIST	00090
	IF (FLSPEC) THEN	HIST	00091
	TAV = CZERO	HIST	00092
	ELSE	HIST	00093
	TAV = CIMAX*TIN	HIST	00094
	END IF	HIST	00095
C		HIST	00096
	CALL RANINT(IRA)	HIST	00097
C		HIST	00098
	IF (IB .EQ. 1) INRAN = IRA	HIST	00101
	DO 130 I = 1, IMAX	HIST	00103
	IHSTRY=I		
	DO 1301 JJJ=1,10		
	EDPR(JJJ)=0.		
	EDNK(JJJ)=0.		
	EDSC(JJJ)=0.		
1301	EDTL(JJJ)=0.		
	IHIST = I	HIST	00104
	MODTMJ = MIN(10000, IMAX)	LAHEY	00017
	IF (I.EQ.MODTMJ*(I/MODTMJ)) THEN	LAHEY	00018

CALL TOTTIM(XTMJ)	LAHEY	00019
WRITE(*, '(/' HISTORY', I8, ', ELAPSED MINUTES', F10.2)')	LAHEY	00020
1I, XTMJ/60.	LAHEY	00021
ENDIF	LAHEY	00022
W = CONE	HIST	00105
CWCF = W	HIST	00106
LAST = 0	HIST	00107
C	HIST	00108
CALL RANSAV(IRSAV)	HIST	00109
C	HIST	00110
C	HIST	00111
C	HIST	00112
C ... SOURCE ENERGY	HIST	00113
C	HIST	00114
IF (FLSPEC) THEN	HIST	00115
RA = RAN(IRAN)	HIST	00116
DO 14 JHIST = 2, JSPEC	HIST	00117
IF ( RA. GT. SPECIN(JHIST) ) GO TO 16	HIST	00118
14 CONTINUE	HIST	00119
16 T = ESP(JHIST-1) + ( RA -SPECIN(JHIST-1) )*( ESP(JHIST)	HIST	00120
\$ - ESP(JHIST-1) )/( SPECIN(JHIST) - SPECIN(JHIST-1) )	HIST	00121
TAV = TAV + T	HIST	00122
IF ( (FLESRC .AND. (T .GT. TCUT) ) .OR.	HIST	00123
\$ (.NOT. FLESRC .AND. (T .GT. TPCUT) ) THEN	HIST	00124
GO TO 20	HIST	00125
ELSE	HIST	00126
NTREJ = NTREJ + 1	HIST	00127
TREJ = TREJ + W*T	HIST	00128
GO TO 1299	HIST	00129
END IF	HIST	00130
END IF	HIST	00131
T = TIN	HIST	00132
20 NT = NTFST	HIST	00133
C	HIST	00134
CALL CLASS (T, NT)	HIST	00135
C	HIST	00136
IF (IDOME.EQ.0) THEN	HIST	00137
C	HIST	00138
C ... SOURCE DIRECTION	HIST	00139
C	HIST	00140
IF (ICTH .EQ. 2) THEN	HIST	00141
RA = RAN(IRAN)	HIST	00142
COM = CTHIN+ RA*(CONE-CTHIN)	HIST	00143
ELSE IF (ICTH .EQ. 3) THEN	HIST	00144
RA = RAN(IRAN)	HIST	00145
COM = SQRT(CTHIN+RA*(CONE-CTHIN))	HIST	00146
ELSE IF (ICTH .EQ. 1) THEN	HIST	00147
CTH(1) = CTSR	HIST	00149
STH(1) = STSR	HIST	00150
CPH(1) = CPSR	HIST	00151
SPH(1) = SPSR	HIST	00153
GO TO 69	HIST	00154
END IF	HIST	00155
C	HIST	00156
IF (CTSR .EQ. CONE) THEN	HIST	00157
CTH(1) = COM	HIST	00159
STH(1) = SQRT(CONE-COM*COM)	HIST	00160
RA = RAN(IRAN)	HIST	00161
JAZ = RA*C360	HIST	00162
CPH(1) = CCH(JAZ+1)	HIST	00163
SPH(1) = SCH(JAZ+1)	HIST	00165
ELSE	HIST	00172
C	HIST	00173
CALL FOLD(CTSR, STSR, CPSR, SPSR, COM, CTH(1), STH(1), CPH(1), SPH(1))	HIST	00174
C	HIST	00176
END IF	HIST	00177
END IF	HIST	00177
C	HIST	00177

C ... SOURCE POSITION

C -----

69 IF (SORCIN .NE. CZERO) THEN

RA = RAN(IRAN)

R = SQRT(RA)\*SORCIN

RA = RAN(IRAN)

JAZ = RA\*C360

SCHR = SCH(JAZ+1)\*R

CCHR = CCH(JAZ+1)\*R

IF (IDISKS .EQ. 0) THEN

X = XSR + CCHR\*W1X+SCHR\*W2X

Y = YSR+CCHR\*W1Y+SCHR\*W2Y

Z = ZSR+CCHR\*W1Z+SCHR\*W2Z

ELSE

IF (KPERPXY.EQ.1) THEN

X = XCENT + CCHR

Y = YCENT + SCHR

Z = ZCENT

END IF

IF (KPERPXZ.EQ.1) THEN

X = XCENT + CCHR

Y = YCENT

Z = ZCENT + SCHR

END IF

IF (KPERPYZ.EQ.1) THEN

X = XCENT

Y = YCENT + CCHR

Z = ZCENT + SCHR

END IF

END IF

ELSE

IF (IRECTS .EQ. 0 .AND. IDOME.EQ.0) THEN

X = XSR

Y = YSR

Z = ZSR

ELSE

IF (IRECTS.NE.0) THEN

RRAA1 = RAN(IRAN)

RRAA2 = RAN(IRAN)

IF (KPERPXY .EQ. 1) THEN

X = XLOWS + RRAA1\*(XHIGHS-XLOWS)

Y = YLOWS + RRAA2\*(YHIGHS-YLOWS)

Z = ZLOWS

END IF

IF (KPERPXZ. EQ. 1) THEN

X = XLOWS + RRAA1\*(XHIGHS-XLOWS)

Y = YLOWS

Z = ZLOWS + RRAA2\*(ZHIGHS-ZLOWS)

END IF

IF (KPERPYZ .EQ.1) THEN

X = XLOWS

HIST 00178

HIST 00179

HIST 00198

HIST 00199

HIST 00200

HIST 00201

HIST 00202

HIST 00203

HIST 00204

HIST 00208

HIST 00209

HIST 00210

HIST 00211



C ... REMOVE SECONDARY ELECTRONS FROM STORAGE FOR TRANSPORT	HIST	00272
C -----	HIST	00273
IF (LAST .NE. 0) THEN	HIST	00274
LB = LBS(LAST)	HIST	00275
Z = ZS(LAST)	HIST	00276
T = TS(LAST)	HIST	00277
NT = NTS(LAST)	HIST	00278
CTH(1) = CTHS(LAST)	HIST	00279
W = WS(LAST)	HIST	00280
IPR = IPRS(LAST)	HIST	00281
C	HIST	00283
X = XS(LAST)	HIST	00284
Y = YS(LAST)	HIST	00285
STH(1) = STHS(LAST)	HIST	00286
CPH(1) = CPHS(LAST)	HIST	00287
SPH(1) = SPHS(LAST)	HIST	00288
C	HIST	00289
LBCZ = LBCS(LAST)	HIST	00291
KLOOP = KLOOP+1	HIST	00292
LAST = LAST-1	HIST	00294
GO TO 70	HIST	00295
END IF	HIST	00296
C	HIST	00297
IF (.NOT. FLPHD) GO TO 1299	HIST	00298
C	HIST	00299
C	HIST	00300
C ... SCORE PULSE-HEIGHT DISTRIBUTION	HIST	00301
C -----	HIST	00302
EABST = CZERO	HIST	00303
DO 100 LS=LPHDB,LPHDE	HIST	00304
EABST = EABST+PHDD(LS)	HIST	00305
100    PHDD(LS) = CZERO	HIST	00306
DO 110 JS=1,JSMAX	HIST	00307
IF (SMARK(JS) .LE. EABST) GO TO 120	HIST	00308
110    CONTINUE	HIST	00309
NPHD = NPHD+1	HIST	00310
GO TO 1299	HIST	00311
120    ABE(JS) = ABE(JS)+CWCF	HIST	00312
1299    IF (NINDV.EQ.0) GO TO 130		
DO 1298 NIND=1,NINDV		
EDTL(NIND)=EDPR(NIND)+EDNK(NIND)+EDSC(NIND)		
1298    CONTINUE		
WRITE(44) (EDPR(NIND), EDNK(NIND), EDSC(NIND), EDTL(NIND), NIND		
\$ =1,NINDV)		
130 CONTINUE	HIST	00313
C	HIST	00314
CALL RANSAV(IRC)	HIST	00315
C	HIST	00316
RETURN	HIST	00317
END	HIST	00318

**APPENDIX 2**  
**CRRES\_D1 Sample Input File for ACCEPT Run**

```

TITLE
  15 MEV DOME SOURCE on CRRES DOME 1
***** GEOMETRY *****
GEOMETRY
*1
  RCC  0.0  0.0  0.0  0.0      0.00000  0.04030  .05093
*2
  RCC  0.0  0.0  -0.07620  0.0    .00000  0.07620  .06350
*3
  RPP  -0.09525  .09525  -0.09525  .09525  .00000  0.04030
*4
  RCC  0.0  0.0  -0.07620  0.0    .00000  0.07620  0.5080
*5
  RCC  0.0  0.0  -0.07620  0.0    .00000  0.07620  1.22936
*6
  RCC  0.0  0.0  -0.07620  0.0    .00000  0.07620  1.46812
*7
  RCC  0.0  0.0  -0.10668  0.0    .00000  0.03048  0.32385
*8
  RCC  0.0  0.0  -0.10668  0.0    .00000  0.03048  1.22936
*9
  RCC  0.0  0.0  -0.10668  0.0    .00000  0.03048  1.46812
*10
  RCC  0.0  0.0  -0.15748  0.0    .00000  0.05080  0.32385
*11
  RCC  0.0  0.0  -0.15748  0.0    .00000  0.05080  1.22936
*12
  RCC  0.0  0.0  -0.15748  0.0    .00000  0.05080  1.46812
*13
  RCC  0.0  0.0  -0.31496  0.0    .00000  0.15748  1.22936
*14
  RCC  0.0  0.0  -0.31496  0.0    .00000  0.15748  1.46812
*15
  RCC  0.0  0.0  -0.94996  0.0    .00000  0.635    1.11125
*16
  RCC  0.0  0.0  -0.94996  0.0    .00000  0.635    1.22936
*17
  RCC  0.0  0.0  -0.94996  0.0    .00000  0.635    1.46812
*18
  RCC  0.0  0.0  -1.58496  0.0    .00000  0.635    1.11125
*19
  RCC  0.0  0.0  -1.58496  0.0    .00000  0.635    1.22936
*20
  RCC  0.0  0.0  -1.58496  0.0    .00000  0.635    1.46812
*21
  RCC  0.0  0.0  0.0      0.0    .00000  1.01981  1.01981
*22
  RCC  0.0  0.0  0.0      0.0    .00000  1.22936  1.22936
*23
  RCC  0.0  0.0  0.0      0.0    .00000  1.46812  1.46812
*24
  SPH  0.0  0.0  0.0  1.01981
*25
  SPH  0.0  0.0  0.0  1.22936
*26
  SPH  0.0  0.0  0.0  1.46812
*27
  RCC  0.0  0.0  -2.58496  0.0  0.0  1.0  1.46812
*28
  SPH  0.0  0.0  0.0  1.005
*29
  RCC  0.0  0.0  0.0  0.0  0.0  1.005  1.005
*30
  SPH  0.0  0.0  0.0  5.0
*31
  SPH  0.0  0.0  0.0      10.0

```

```

END
*SI
  Z01 +1
  Z02 +3 -1
*VOID
  Z03 +29 +28 -1 -3
*AL
  Z04 +25 -24 +22
  Z05 +5 -4 -2
*VOID
  z06 +6 -5 -4 -2
*AL203
  Z07 +4 -2
*VOID
  Z08 +2
*AL
  Z09 +8 -7
*VOID
  z10 +9 -8 -7
  Z11 +7
  z12 +12 -11 -10
*AL
  Z13 +11 -10
*NI
  Z14 +10
*AL
  Z15 +13
*VOID
  z16 +14 -13
  z17 +17 -16
*AL
  z18 +16 -15
  z19 +19 -18
*W-Fe
  Z20 +15
  z21 +18
*AL
  z22 +20 -19
*VOID
  Z23 +24 -28 +21
  Z24 +23 -25 +26
  z25 +23 -26
  Z26 +27
  Z27 +29 -1 -2 -3 -4 -5 -6 -7 -8 -9 -10 -11 -12 -13 -14 -15
    -16 -17 -18 -19 -20 -21 -22 -23 -24 -25 -26 -27 -28
  Z28 +30 -29
END
*MATERIAL
1
1
0
2
2
0
3
0
2
0
0
0
0
2
4
2
0
0
2
2
5
5
2
0
0

```

```

0
0
0
0
***** SOURCE *****
ELECTRONS
ENERGY 15.0
***** OPTIONS *****
PULSE-HEIGHT 1 1
  NBINE 34 USER
14.99999 10.1 9.57 8.94 8.3 7.67 7.01 6.37 5.74 5.12 4.48 3.84
3.2 2.56 1.91 1.28
1.020 0.979 0.910 0.839 0.765 0.694 0.622 0.549 0.480
0.408 0.336 0.263 0.193 0.125 0.051 0.049 0.00001 0.0
ELECTRON-FLUX 1 1
  NBINE 19 USER
14.99999 1.020 0.979 0.910 0.839 0.765 0.694 0.622 0.549 0.480
0.408 0.336 0.263 0.193 0.125 0.051 0.049 0.00001 0.0
DOME-SOURCE 0. 0. 0.0 1.25
***** OPTIONS *****
CUTOFFS 0.1 0.01
HISTORIES 1000000

```





### APPENDIX 3

#### CEASE Telescope - MCNPX Flat Disk Proton Source Runs

**MCNPX Run 1.** Disc source located at  $z=0.457$  cm along telescope axis;  
 disk source radius = 0.025 cm;  
 9 MeV proton source  
 10,000 histories  
 Partial listing of output file: input file image, pulse height, flux, and energy deposition for  
 cells 67 (DFT) and 88 (DBT)

```

1-      Test for protons  CEASE Flight Sensor 9 MeV rad=0.025cm
2-      C
3-      C   Proton
4-      C   transport - disk source, 9 MeV proton 40 deg slant  at z=.4572
  
```

GEOMETRY FILE DETAILS SAME AS SHOWN IN [FIRST YEAR REPORT]APPENDIX 3 OMITTED HERE FOR BREVITY

```

462-      C
463-      c   Transport protons, neutrons, muons, photons, pions, kaons,
464-      c   deuterons, alphas
465-
466-      mode  h
467-      cut:h 1.e+8 0.05
468-      c   mode  h n | p /
469-      c   Source definition, proton source (par=9), located on surface
470-      c   #47 which is the plane at z=0.4572, centered at 0.,0.,0.4572,
471-      c   with radius 0.025 cm, energy 9 MeV,40deg slant incidence (along z)
472-      SDEF  sur=47 pos=0. 0. .4572 rad=D1 ERG=9. WGT=1.0 par=9
473-      dir=0.7660444
474-      SI1  .025
475-      VOL  45J 0.144715 3J 4.501818 27J 0.1311943 21J 0.1333961
476-      2J 0.1129316 0.4679637 14J 19.61581 61.74832 5J
477-      139.2479 139.2432 103.1126 103.1126 103.1126
478-      103.1126 42J
479-      c   No. of histories
480-      NPS  10000
481-      C
482-      C   Materials
483-      C
484-      C   Brass
485-      M1  29000 -.3 28000 -.7
486-      C   Aluminum
487-      M2  13027 -1.0
488-      C   Tungsten
489-      M3  74000 -.95 29000 -.015 28000 -.035
490-      C   Gold
491-      M4  79197 -1.0
492-      C   Stainless Steel
493-      M5  26000 -.71 29000 -.17 25055 -.065 28000 -.005 14000 -.05
494-      C   Conductive Silicone Elastomer
495-      M6  28000 -.377 47000 -.373 14000 -.0947
496-      6000 -.0810 8016 -.0539 1001 -.0204
497-      C   PMMA
498-      M7  6000 -.59985 8016 -.31961 1001 -.080538
499-      C   Silicon
500-      M8  14000 -1.0
501-      C   Copper
502-      M9  29000 -1.0
503-      C
504-      C
505-      C
506-      c   maximum proton energy(MeV) required for cross section table
507-      PHYS:h 10.
508-      c   maximum neutron energy(MeV) required for cross section table
509-      PHYS:n 10.
510-      c   maximum muon energy(MeV) required for cross section table
511-      PHYS:| 10.
512-      c   maximum photon energy(MeV) required for cross section table
513-      PHYS:p 10.
514-      c   maximum pion energy(MeV) required for cross section table
515-      PHYS:/ 10.
516-      c
  
```

```

517- c Tallies
518- c proton pulse height tallies
519- F8:h 67
520- E8 0 1.e-5 .5 1. 1.5 2. 2.3 3. 3.5 4. 4.5 5. 5.5 6. 6.5
521- 7. 7.5 8. 8.5 8.99999 9.
522- F38:h 88
523- E38 0 1.e-5 .5 1. 1.5 2. 2.3 3. 3.5 4. 4.5 5. 5.5 6. 6.5
524- 7. 7.5 8. 8.5 8.99999 9.
525- c proton energy deposition tallies
526- *F18:h 67 88
527- c proton flux tallies
528- F44:h 67 88
529- c c proton energy flux tallies
530- *F104:h 67 88
531- c cell importances for protons
532- imp:h 1 165R 0 6R
533- c cell importances for photons
534- c imp:p 1 165R 0 6R
535- c cell importances for neutrons
536- c imp:n 1 165R 0 6R
537- c cell importances for muons
538- c imp:| 1 165R 0 6R
539- c cell importances for pions
540- c imp:/ 1 165R 0 6R
541-

```

```

ltally 8 nps = 10000
tally type 8 pulse height distribution. units number
particle(s): proton

```

```

cell 67
energy
0.0000E+00 0.0000E+00 0.0000
1.0000E-05 0.0000E+00 0.0000
5.0000E-01 1.0000E-03 0.3161
1.0000E+00 3.2000E-03 0.1765
1.5000E+00 2.9000E-03 0.1854
2.0000E+00 5.1300E-02 0.0430
2.3000E+00 2.7100E-02 0.0599
3.0000E+00 3.4100E-02 0.0532
3.5000E+00 1.6200E-02 0.0779
4.0000E+00 1.2200E-02 0.0900
4.5000E+00 1.0300E-02 0.0980
5.0000E+00 3.9000E-03 0.1598
5.5000E+00 1.1000E-03 0.3013
6.0000E+00 1.0000E-04 0.9999
6.5000E+00 0.0000E+00 0.0000
7.0000E+00 0.0000E+00 0.0000
7.5000E+00 0.0000E+00 0.0000
8.0000E+00 0.0000E+00 0.0000
8.5000E+00 0.0000E+00 0.0000
9.0000E+00 0.0000E+00 0.0000
9.0000E+00 0.0000E+00 0.0000
total 1.6340E-01 0.0226
tally type 8* energy deposition units mev
particle(s): proton

```

```

cell 67
4.15596E-01 0.0243

```

```

cell 88
2.61874E-02 0.1198
tally type 8 pulse height distribution. units number
particle(s): proton

```

```

cell 88
energy
0.0000E+00 0.0000E+00 0.0000
1.0000E-05 0.0000E+00 0.0000
5.0000E-01 2.0000E-04 0.7070
1.0000E+00 8.0000E-04 0.3534
1.5000E+00 7.0000E-04 0.3778
2.0000E+00 3.0000E-04 0.5773
2.3000E+00 5.0000E-04 0.4471
3.0000E+00 1.4000E-03 0.2671
3.5000E+00 1.2000E-03 0.2885
4.0000E+00 1.0000E-03 0.3161
4.5000E+00 8.0000E-04 0.3534
5.0000E+00 6.0000E-04 0.4081
5.5000E+00 5.0000E-04 0.4471
6.0000E+00 4.0000E-04 0.4999
6.5000E+00 1.0000E-04 0.9999
7.0000E+00 0.0000E+00 0.0000
7.5000E+00 0.0000E+00 0.0000

```

```

8.0000E+00  0.00000E+00  0.0000
8.5000E+00  0.00000E+00  0.0000
9.0000E+00  0.00000E+00  0.0000
9.0000E+00  0.00000E+00  0.0000
total       8.50000E-03  0.1080
tally type 4 track length estimate of particle flux.      units  1/cm**2
particle(s): proton

volumes
cell:        67          88
            7.61920E-03  4.23017E-02
cell 67
            3.57828E-01  0.0241
cell 88
            2.20099E-03  0.1326
tally type 4* track length estimate of energy flux.      units  mev/cm**2
particle(s): proton
volumes
cell:        67          88
            7.61920E-03  4.23017E-02
cell 67
            2.02689E+00  0.0268
cell 88
            5.68473E-03  0.1553
Test for protons CEASE Flight Sensor 9 MeV
rad=0.025cm
C

```

---

**MCNPX Run 2.** Disc source located at  $z=0.457$  cm along telescope axis;  
 disk source radius = 0.050 cm;  
 9 MeV proton source  
 40,000 histories  
 Partial listing of output file: input file image, pulse height, flux, and energy deposition for  
 cells 67 (DFT) and 88 (DBT)

```

1- Test for protons CEASE Flight Sensor 9 MeV rad=0.05cm
2- C
3- C Proton
4- C transport - disk source, 9 MeV proton 40 deg slant at z=.4572
5- C
462- C
463- c Transport protons, neutrons, muons, photons, pions, kaons,
464- c deuterons, alphas
465-
466- mode h
467- cut:h 1.e+8 0.05
468- c mode h n | p /
469- c Source definition, proton source (par=9), located on surface
470- c #47 which is the plane at z=0.4572, centered at 0.,0.,0.4572,
471- c with radius 0.05 cm, energy 9 MeV,40deg slant incidence (along z)
472- SDEF sur=47 pos=0. 0. .4572 rad=D1 ERG=9. WGT=1.0 par=9
473- dir=0.7660444
474- SI1 .05
475- VOL 45J 0.144715 3J 4.501818 27J 0.1311943 21J 0.1333961
476- 2J 0.1129316 0.4679637 14J 19.61581 61.74832 5J
477- 139.2479 139.2432 103.1126 103.1126 103.1126
478- 103.1126 42J
479- c No. of histories
480- NPS 40000
481- C

```

```

482- C Materials
483- C
484- C Brass
485- M1 29000 -.3 28000 -.7
486- C Aluminum
487- M2 13027 -1.0
488- C Tungsten
489- M3 74000 -.95 29000 -.015 28000 -.035
490- C Gold
491- M4 79197 -1.0
492- C Stainless Steel
493- M5 26000 -.71 29000 -.17 25055 -.065 28000 -.005 14000 -.05
494- C Conductive Silicone Elastomer
495- M6 28000 -.377 47000 -.373 14000 -.0947
496- C 6000 -.0810 8016 -.0539 1001 -.0204
497- C PMMA
498- M7 6000 -.59985 8016 -.31961 1001 -.080538
499- C Silicon
500- M8 14000 -1.0
501- C Copper
502- M9 29000 -1.0
503- C
504- C
505- C
506- c maximum proton energy(MeV) required for cross section table
507- PHYS:h 10.
508- c maximum neutron energy(MeV) required for cross section table
509- PHYS:n 10.
510- c maximum muon energy(MeV) required for cross section table
511- PHYS:| 10.
512- c maximum photon energy(MeV) required for cross section table
513- PHYS:p 10.
514- c maximum pion energy(MeV) required for cross section table
515- PHYS:/ 10.
516- c
517- c Tallies
518- c proton pulse height tallies
519- F8:h 67
520- E8 0 1.e-5 .5 1. 1.5 2. 2.3 3. 3.5 4. 4.5 5. 5.5 6. 6.5
521- 7. 7.5 8. 8.5 8.99999 9.
522- F38:h 88
523- E38 0 1.e-5 .5 1. 1.5 2. 2.3 3. 3.5 4. 4.5 5. 5.5 6. 6.5
524- 7. 7.5 8. 8.5 8.99999 9.
525- c proton energy deposition tallies
526- *F18:h 67 88
527- c proton flux tallies
528- F44:h 67 88
529- c c proton energy flux tallies
530- *F104:h 67 88
531- c cell importances for protons
532- imp:h 1 165R 0 6R
533- c cell importances for photons
534- c imp:p 1 165R 0 6R
535- c cell importances for neutrons
536- c imp:n 1 165R 0 6R
537- c cell importances for muons
538- c imp:| 1 165R 0 6R
539- c cell importances for pions
540- c imp:/ 1 165R 0 6R
541-

```

```

ltally 8 nps = 40000
tally type 8 pulse height distribution. units number
particle(s): proton

```

```

cell 67
energy
0.0000E+00 0.00000E+00 0.0000
1.0000E-05 0.00000E+00 0.0000
5.0000E-01 5.75000E-04 0.2085
1.0000E+00 1.45000E-03 0.1312
1.5000E+00 1.90000E-03 0.1146
2.0000E+00 1.49500E-02 0.0406
2.3000E+00 1.01750E-02 0.0493
3.0000E+00 1.61250E-02 0.0391
3.5000E+00 7.27500E-03 0.0584
4.0000E+00 5.50000E-03 0.0672
4.5000E+00 4.72500E-03 0.0726
5.0000E+00 1.80000E-03 0.1177
5.5000E+00 2.00000E-04 0.3535
6.0000E+00 0.00000E+00 0.0000

```

6.5000E+00	0.00000E+00	0.0000		
7.0000E+00	0.00000E+00	0.0000		
7.5000E+00	0.00000E+00	0.0000		
8.0000E+00	0.00000E+00	0.0000		
8.5000E+00	0.00000E+00	0.0000		
9.0000E+00	2.50000E-05	1.0000		
9.0000E+00	0.00000E+00	0.0000		
total	6.47000E-02	0.0190		
	tally type 8*	energy deposition	units	mev
	particle(s):	proton		
cell 67				
	1.69238E-01	0.0202		
cell 88				
	1.30129E-02	0.0846		
	tally type 8	pulse height distribution.	units	number
	particle(s):	proton		
cell 88				
	energy			
0.0000E+00	0.00000E+00	0.0000		
1.0000E-05	0.00000E+00	0.0000		
5.0000E-01	2.50000E-04	0.3162		
1.0000E+00	3.00000E-04	0.2886		
1.5000E+00	3.00000E-04	0.2886		
2.0000E+00	5.00000E-04	0.2236		
2.3000E+00	2.50000E-04	0.3162		
3.0000E+00	9.25000E-04	0.1643		
3.5000E+00	4.75000E-04	0.2294		
4.0000E+00	3.00000E-04	0.2886		
4.5000E+00	3.25000E-04	0.2773		
5.0000E+00	3.00000E-04	0.2886		
5.5000E+00	2.50000E-04	0.3162		
6.0000E+00	2.00000E-04	0.3535		
6.5000E+00	7.50000E-05	0.5773		
7.0000E+00	0.00000E+00	0.0000		
7.5000E+00	0.00000E+00	0.0000		
8.0000E+00	0.00000E+00	0.0000		
8.5000E+00	0.00000E+00	0.0000		
9.0000E+00	0.00000E+00	0.0000		
9.0000E+00	0.00000E+00	0.0000		
total	4.45000E-03	0.0748		
	tally type 4	track length estimate of particle flux.	units	1/cm**2
	particle(s):	proton		
	volumes			
	cell:	67 88		
		7.61920E-03 4.23017E-02		
cell 67				
	1.35987E-01	0.0203		
cell 88				
	1.08395E-03	0.0956		
	tally type 4*	track length estimate of energy flux.	units	mev/cm**2
	particle(s):	proton		
	volumes			
	cell:	67 88		
		7.61920E-03 4.23017E-02		
cell 67				
	7.09309E-01	0.0227		
cell 88				
	2.81644E-03	0.1149		

2  
3  
4  
5

6  
7  
8  
9

**APPENDIX 4**  
**MCNPX Output File for Grazing Angle Proton Scattering Study**  
**250 keV Proton Beam Incident on Iridium Slab, Angle of Incidence = 0.1°**

1mcnpX version 2.1.5 ld=Fri May 21 09:49:28 MDT 1999 11/21/01 11:48:39 11/21/01 11:48:39  
 \*\*\*\*\*  
 imp=ird250p1 out=oir250p1 \*\*\*\*\* probid =

\*  
 \*  
 \*  
 \*  
 \*

Grazing incident proton beam on Iridium slab 250 keV

1-	C	Cells
2-	C	Iridium slab
3-	1	1 -22.42 1 -2 3 -4 5 -6
4-	C	Void region above slab
5-	2	0 2 -7 3 -4 5 -6
6-	C	escape
7-	3	0 -1.7:-3.4:-5.6
8-		
9-		
10-	C	Surfaces
11-	1	pz -1.0
12-	2	pz 0.0
13-	3	px -3.0
14-	4	px 3.0
15-	5	py -1.0
16-	6	py 4.0
17-	7	pz 1.0
18-	C	
19-		
20-	C	Transport protons
21-	mode	h
22-	C	
23-	C	Source defined by subroutine srcoblq.F is a monodirectional
24-	C	beam source grazing incidence 90.1 degrees off normal
25-	C	Energy is 0.25 MeV
26-	C	
27-	C	
28-	C	no. of histories





LAHET energy cutoff settings:

```

emin() =
1.00000E+03 1.00000E+30 1.00000E+30 1.00000E+30 1.00000E+30 1.00000E+30
1.00000E+30 1.00000E+30 1.00000E+30 1.00000E+30 1.00000E+30 1.00000E+30
1.00000E+30 1.00000E+30 1.00000E+30 1.00000E+30 1.00000E+30 1.00000E+30
1.00000E+30
  
```

print table 41

LAHET physics options:

```

lca ielas ipreq iexisa ichoic jcoul nexite npidk noact icem
lca 2 1 1 23 1 1 0 0 1 0
lcb flenb(i),i=1,6
lcb 3.4900E+03 3.4900E+03 2.4900E+03 2.4900E+03 8.0000E+02 8.0000E+02 -1.0000E+00 -1.0000E+00
ctofe flim0
lea ipht icc nobalc nobale ifbrk ilvden ievap nofis
lea 1 4 1 0 1 0 0 1
leby zere bzero
leby 1.5000E+00 8.0000E+00 1.5000E+00 1.0000E+01
  
```

print table 60

1cells

cell	mat	atom density	gram density	volume	mass	pieces	proton importance
1	1	7.02409E-02	2.24200E+01	3.00000E+01	6.72600E+02	0	1.0000E+00
2	0	0.00000E+00	0.00000E+00	3.00000E+01	0.00000E+00	0	1.0000E+00
3	0	0.00000E+00	0.00000E+00	0.00000E+00	0.00000E+00	0	0.0000E+00

total 6.00000E+01 6.72600E+02

1 warning message so far.

decimal words of dynamically allocated storage

```

general 37806
tallies 31228
bank 19703
cross sections 0
  
```

total 81009 = 324036 bytes

available (mdas) 4000000

1problem summary

run terminated when 10000000 particle histories were done.

+ Grazing incident proton beam on Iridium slab 250 keV

probid = 11/22/01 18:52:54

0 11/21/01 11:48:39

proton creation	tracks	weight (per source particle)	energy (per source particle)	proton loss	tracks	weight (per source particle)	energy (per source particle)

```

source          100000000  1.0000E+00  2.5000E-01  85340666  8.5341E-01  1.9430E-01
nucl. interaction 0 0. 0. 14659334 1.4659E-01 1.4659E-04
particle decay 0 0. 0. 0 0. 0.
weight window 0 0. 0. 0 0. 0.
cell importance 0 0. 0. 0 0. 0.
weight cutoff 0 0. 0. 0 0. 0.
energy importance 0 0. 0. 0 0. 0.
dxtran 0 0. 0. 0 0. 0.
forced collisions 0 0. 0. 0 0. 0.
exp. transform 0 0. 0. 0 0. 0.
tabular sampling 0 0. 0. 0 0. 5.5550E-02

elastic recoil 0 0. 0. 0 0. 0.
total 100000000 1.0000E+00 2.5000E-01 100000000 1.0000E+00 2.5000E-01

```

```

computer time so far in this run 1596.25 minutes 0
computer time in mcrun 1596.23 minutes 0
source particles per minute 6.2647E+04 324052 bytes.
random numbers generated 53634305630 4326 in history 70074867

```

```

range of sampled source weights = 1.0000E+00 to 1.0000E+00
1p proton activity in each cell

```

cell	tracks entering	population	substeps	substeps * weight (per history)	flux weighted energy	average track weight (relative)	average track mfp (cm)
1	100000000	100000000	10796091450	1.0796E+02	1.3716E-01	1.0000E+00	4.4749E-07
2	185340666	100000000	0	0.0000E+00	2.3315E-01	1.0000E+00	0.0000E+00
total	285340666	200000000	10796091450	1.0796E+02			

tally 1 nps = 100000000  
tally type 1 number of particles crossing a surface.  
particle(s): proton

```

surface 2
cosine bin: -1. to 0.0000E+00
energy
1.2500E-02 0.0000E+00 0.0000
2.5000E-02 0.0000E+00 0.0000
3.7500E-02 0.0000E+00 0.0000
5.0000E-02 0.0000E+00 0.0000
6.2500E-02 0.0000E+00 0.0000

```

7.5000E-02	0.0000E+00	0.0000
8.7500E-02	0.0000E+00	0.0000
1.0000E-01	0.0000E+00	0.0000
1.1250E-01	0.0000E+00	0.0000
1.2500E-01	0.0000E+00	0.0000
1.3750E-01	0.0000E+00	0.0000
1.5000E-01	0.0000E+00	0.0000
1.6250E-01	0.0000E+00	0.0000
1.7500E-01	0.0000E+00	0.0000
1.8750E-01	0.0000E+00	0.0000
2.0000E-01	0.0000E+00	0.0000
2.1250E-01	0.0000E+00	0.0000
2.2500E-01	0.0000E+00	0.0000
2.3750E-01	0.0000E+00	0.0000
2.5000E-01	1.0000E+00	0.0000
total	1.0000E+00	0.0000

20 energy bins

Angle bin #1, 0°-0.1°  
(cosine shown is  $\cos(\pi/2 - \theta)$ )

surface 2  
cosine bin: 0.0000E+00 to 1.74530E-03

energy		
1.2500E-02	2.0000E-07	0.2236
2.5000E-02	3.8000E-07	0.1622
3.7500E-02	4.4000E-07	0.1508
5.0000E-02	4.2000E-07	0.1543
6.2500E-02	2.5000E-07	0.2000
7.5000E-02	4.6000E-07	0.1474
8.7500E-02	3.2000E-07	0.1768
1.0000E-01	5.3000E-07	0.1374
1.1250E-01	5.3000E-07	0.1374
1.2500E-01	7.1000E-07	0.1187
1.3750E-01	9.0000E-07	0.1054
1.5000E-01	1.3700E-06	0.0854
1.6250E-01	2.1500E-06	0.0682
1.7500E-01	3.0900E-06	0.0569
1.8750E-01	4.7700E-06	0.0458
2.0000E-01	8.6600E-06	0.0340
2.1250E-01	1.5870E-05	0.0251
2.2500E-01	4.2090E-05	0.0154
2.3750E-01	1.6972E-04	0.0077
2.5000E-01	5.6062E-03	0.0013
total	5.85913E-03	0.0013

\*  
\*  
\*  
\*  
\*

surface 2  
cosine bin: 9.84810E-01 to 9.96190E-01

energy	
1.2500E-02	1.56000E-05 0.0253
2.5000E-02	7.27300E-05 0.0117
3.7500E-02	1.13430E-04 0.0094
5.0000E-02	1.30160E-04 0.0088
6.2500E-02	1.20160E-04 0.0091
7.5000E-02	9.04100E-05 0.0105
8.7500E-02	5.75000E-05 0.0132
1.0000E-01	2.97200E-05 0.0183
1.1250E-01	1.18700E-05 0.0290
1.2500E-01	3.82000E-06 0.0512
1.3750E-01	9.30000E-07 0.1037
1.5000E-01	1.10000E-07 0.3015
1.6250E-01	1.00000E-08 1.0000
1.7500E-01	0.00000E+00 0.0000
1.8750E-01	0.00000E+00 0.0000
2.0000E-01	0.00000E+00 0.0000
2.1250E-01	0.00000E+00 0.0000
2.2500E-01	0.00000E+00 0.0000
2.3750E-01	0.00000E+00 0.0000
2.5000E-01	0.00000E+00 0.0000
total	6.46450E-04 0.0039

Angle bin #68,  
85°-90°

surface 2  
cosine bin: 9.96190E-01 to 1.00000E+00

energy	
1.2500E-02	5.49000E-06 0.0427
2.5000E-02	2.38600E-05 0.0205
3.7500E-02	3.82600E-05 0.0162
5.0000E-02	4.36400E-05 0.0151
6.2500E-02	4.06900E-05 0.0157
7.5000E-02	2.92400E-05 0.0185
8.7500E-02	1.79600E-05 0.0236
1.0000E-01	8.39000E-06 0.0345
1.1250E-01	3.58000E-06 0.0529
1.2500E-01	9.50000E-07 0.1026
1.3750E-01	1.80000E-07 0.2357
1.5000E-01	4.00000E-08 0.5000
1.6250E-01	0.00000E+00 0.0000
1.7500E-01	0.00000E+00 0.0000
1.8750E-01	0.00000E+00 0.0000
2.0000E-01	0.00000E+00 0.0000
2.1250E-01	0.00000E+00 0.0000
2.2500E-01	0.00000E+00 0.0000
2.3750E-01	0.00000E+00 0.0000

2.5000E-01 0.00000E+00 0.0000  
 total 2.12280E-04 0.0069

\*  
 \*  
 \*  
 \*  
 \*  
 \*

tally type 1 number of particles crossing a surface.  
 particle(s): proton

surface 2  
 cosine bin: -1. to 0.00000E+00  
 energy  
 1.2500E-02 0.00000E+00 0.0000  
 2.5000E-02 0.00000E+00 0.0000  
 3.7500E-02 0.00000E+00 0.0000  
 5.0000E-02 0.00000E+00 0.0000  
 6.2500E-02 0.00000E+00 0.0000  
 7.5000E-02 0.00000E+00 0.0000  
 8.7500E-02 0.00000E+00 0.0000  
 1.0000E-01 0.00000E+00 0.0000  
 1.1250E-01 0.00000E+00 0.0000  
 1.2500E-01 0.00000E+00 0.0000  
 1.3750E-01 0.00000E+00 0.0000  
 1.5000E-01 0.00000E+00 0.0000  
 1.6250E-01 0.00000E+00 0.0000  
 1.7500E-01 0.00000E+00 0.0000  
 1.8750E-01 0.00000E+00 0.0000  
 2.0000E-01 0.00000E+00 0.0000  
 2.1250E-01 0.00000E+00 0.0000  
 2.2500E-01 0.00000E+00 0.0000  
 2.3750E-01 0.00000E+00 0.0000  
 2.5000E-01 1.00000E+00 0.0000  
 total 1.00000E+00 0.0000

surface 2  
 cosine bin: 0.00000E+00 to 1.00000E+00  
 energy  
 1.2500E-02 6.56210E-04 0.0039  
 2.5000E-02 2.65809E-03 0.0019  
 3.7500E-02 4.23233E-03 0.0015

Sum over all  
 angle bins

```

5.0000E-02 4.96509E-03 0.0014
6.2500E-02 5.44576E-03 0.0014
7.5000E-02 5.55055E-03 0.0013
8.7500E-02 5.79733E-03 0.0013
1.0000E-01 5.91880E-03 0.0013
1.1250E-01 6.39339E-03 0.0012
1.2500E-01 6.80390E-03 0.0012
1.3750E-01 7.32951E-03 0.0012
1.5000E-01 8.16091E-03 0.0011
1.6250E-01 9.29315E-03 0.0010
1.7500E-01 1.08095E-02 0.0010
1.8750E-01 1.28450E-02 0.0009
2.0000E-01 1.61703E-02 0.0008
2.1250E-01 2.21435E-02 0.0007
2.2500E-01 3.40218E-02 0.0005
2.3750E-01 6.65577E-02 0.0004
2.5000E-01 6.17654E-01 0.0001
total 8.53407E-01 0.0000

```

```

*
*
*
*
*

```

run terminated when 100000000 particle histories were done.

computer time = 1596.25 minutes

mcpnx version 2.1.5 Fri May 21 09:49:28 MDT 1999

11/22/01 18:52:55

probid = 11/21/01 11:48:39

## APPENDIX 5

### MCNPX Source Subroutine for Grazing Angle Proton Scattering Study

```
c_deck so source
so      1
        subroutine source
so      2
c      user supplied source subroutine
#include "cm.h"
c
c      This is the source routine for oblique proton beams
c      incident on Al or Ir slab
c      The name of this deck is srcoblq.F
c
        data pin/3.14159265/
        data komin/0/
        if(komin.eq.0)then
            komin=1
            open(47,form='unformatted',status='scratch')
            write(jtty,20)
20      format(1x,'Enter source energy (MeV) and incident
obliquity (deg.)
        $')
c      example, 2 degree obliquity means enter 92.0 deg (i.e.
92 deg off normal)
            read(itty,*)erg,obliq
            write(47)erg,obliq
            write(jtty,21)erg,obliq
            write(iuo,21)erg,obliq
21      format(1x,'Source energy (MeV)=' ,e12.5,2x,'Incident
obliquity (deg
        $.) =' ,e12.5)
            rewind 47
            end if
            wgt=1.0
            tme=0.0
            read(47)erg,obliq
            rewind 47
c
c      The source energy
c      erg= 0.1
c      ipt=9 denotes proton source.
c
            ipt=9
c      incident grazing obliquity 92 degrees off normal (2
degrees off surface)
            ths=obliq/180.*pin
            sths=sin(ths)
            cths=cos(ths)
c      incident azimuth = 90 degrees
            phs=0.5*pin
            sphs=1.0
            cphs=0.0
```



```
c    direction cosines of incident beam
    uuu=sths*cphs
    vvv=sths*sphs
    www=cths
    aa=sqrt(uuu**2+vvv**2+www**2)
    uuu=uuu/aa
    vvv=vvv/aa
    www=www/aa
c    point of source incidence
    xxx=0.0
    yyy=-0.99
    zzz=yyy*cths/sths
    jsu=0
    icl=2
    do 50 ispr=1,3
50   spare(ispr)=0.0
    return
    end
```

## APPENDIX 6

### PHILOOK, Program for Extraction and Conversion to Histogram Form of Emergent Proton Azimuthal Distributions from MCNPX PTRAC File Output Produced in the Grazing Angle Proton Scattering Study

```
implicit real*8 (a-h,o-z)
dimension phibin(60),count(60),a(200),b(200)
character*120 line
data pye/3.14159265/
data count/60*0./
open(2,file='lookit',status='unknown')
open(7,file='bin1',status='unknown')
write(6,1)
1   format(1x,'Enter number of phi bins and number of
histories')
   read(5,*)nbins,hists
   dphi=360./nbins
   write(6,17)nbins
17  format(1x,i5)
   phibin(1)=dphi
   do 10 n=2,nbins
10  phibin(n)=phibin(n-1)+dphi
   fac=180./pye
   open(1,file='ptrac',status='old')
   do 20 i=1,10
20  read(1,2)line
   2   format(a)
100 read(1,2,end=200)line
   read(1,2)line
   read(1,*)x,y,z,u,v,w,e,wt,t
   sth=sqrt(1.-w*w)
   if(sth.eq.0.)go to 100
   cphi=u/sth
   sphi=v/sth
   if(cphi.ge.0. .and. sphi.ge.0.)kq=1
   if(cphi.ge.0. .and. sphi.lt.0.)kq=4
   if(cphi.lt.0. .and. sphi.ge.0.)kq=2
   if(cphi.lt.0. .and. sphi.lt.0.)kq=3
   if(abs(sphi-1.0) .le.1.e-5)kq=5
   if(kq.eq.5)phi=0.5*pye
   if(kq.eq.1)phi=asin(abs(sphi))
   if(kq.eq.2)phi=pye-asin(abs(sphi))
   if(kq.eq.3)phi=pye+asin(abs(sphi))
   if(kq.eq.4)phi=2.*pye-asin(abs(sphi))
   phid=fac*phi
   do 30 n=1,nbins
```

```

        if(phid.gt.phibin(n))go to 30
        ibin=n
        if(ibin.eq.1)write(7,77)x,y,z,u,v,w,sphi,cphi
77      format(1x,8e16.9)
        count(ibin)=count(ibin)+1.
        go to 100
30      continue
200     do 210 n=1,nbins
        count(n)=count(n)/hists
210     write(2,4)n,phibin(n),count(n)
4       format(1x,'bin no.=' ,i5,1x,'upper
bound(deg.)=' ,f7.2,1x,'count=' ,e
        $12.5)
        i=1
        a(1)=0.
        b(1)=count(1)
        nb1=nbins-1
        do 215 n=1,nb1
        i=i+1
        a(i)=phibin(n)
        b(i)=count(n)
        i=i+1
        a(i)=phibin(n)
215     b(i)=count(n+1)
        ii=i+1
        a(ii)=360.
        b(ii)=b(1)
        do 220 i=1,ii
220     write(2,5)a(i),b(i)
5       format(1x,f7.1, 2x,e12.5)
        close (1)
        close (2)
        stop
        end

```